This article has been accepted for publication in IEEE Transactions on Wireless Communications. This is the author's version which has not been fully edited and content may change prior to final publication. Citation information: DOI 10.1109/TWC.2025.3563828

Relay Incentive Mechanisms Using Wireless Power Transfer in Non-Cooperative Networks

Winston Hurst, *Student Member, IEEE,* and Yasamin Mostofi, *Fellow, IEEE*

***Abstract*—The advances of 6G systems have prompted the study of new communication paradigms, including relay networks enabled by wireless power transfer (WPT). While existing literature focuses on the cooperative case, this paper examines a non-cooperative scenario in which a source must incentivize one of several battery-powered user equipments (UEs) to act as a relay by offering payment in the form of WPT, while the utility-maximizing UEs seeking to extract as much energy from the source as possible. We propose a protocol based on a reverse auction that enables the source to determine which candidate UE to select as the relay and the amount of energy to be transferred as payment, even when the channel quality between the candidates and the destination is unknown to the source. We first examine the performance of the system under the classical Vickrey auction. We prove that our protocol achieves the best possible outage probability and point out ways to mitigate the gap in energy efficiency when compared to a cooperative baseline. We then analyze system performance under a Myerson auction, which maximizes the auctioneer's utility. To ensure computational tractability, we extend the forward auction regularity condition to the reverse setting, providing a mathematical characterization of regularity and the associated pricing mechanism. We then prove the regularity of the WPT-based auction under both lognormal and Rayleigh fading. To validate our analytical findings, we present extensive numerical results demonstrating how system parameters affect energy efficiency and outage probability. Our results show that auction-based protocols can reduce both outage probability and communication energy by more than 50% with as few as two relay candidates, compared to direct transmission by the source. Additionally, they demonstrate exponential convergence to the cooperative lower performance bound and indicate conditions under which one auction type is preferred over the other. Overall, the auction-based system offers a foundation for improved energy efficiency and communication reliability in non-cooperative environments.**

I. Introduction

As 6G standards come into clearer focus, a number of key technologies, paradigms, and challenges have received increasing attention [1]. Higher communication frequencies, including mmWave and THz communications, will enable massive data rates, but they will also require new network topographies to account for propagation phenomena, such as high penetration loss and sparse multipath effects, not commonly present at lower frequencies [2]. As the number of connected devices continues to grow rapidly, there is increased demand for distributed architectures and frameworks, such as federated learning and edge computing, that avoid the overhead of fully centralized systems [3, 4]. Wireless power transfer (WPT) has also received attention as a potential enabler for networks of unpowered sensors, among other applications [5, 6]. Finally, running as a common thread through all these trends is the need to keep systems energy efficient, particularly in the face of climate change [7].

Winston Hurst and Yasamin Mostofi are with the Department of Electrical and Computer Engineering, University of California, Santa Barbara, USA (email: {winstonhurst, ymostofi}@ece.ucsb.edu). This work was supported in part by ONR award N00014-23-1-2715.

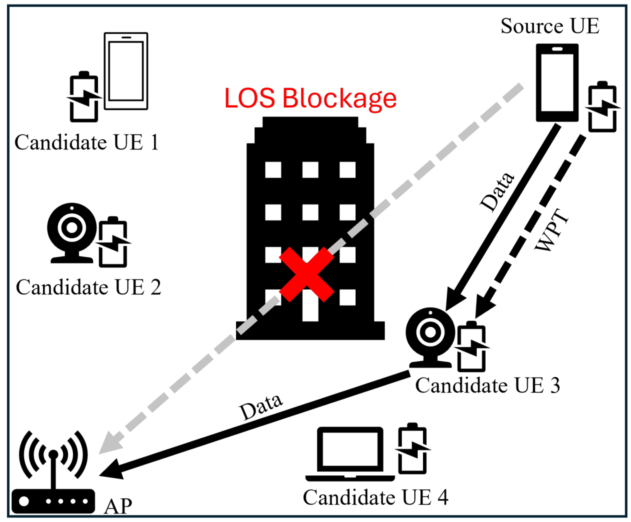

Fig. 1. Overview of problem scenario. A source UE must offload data to the AP, but the LOS path is blocked, resulting in poor link quality. The source must induce a candidate UE to cooperate with a payment in the form of WPT.

In this paper, we examine a scenario at the confluence of these factors. Specifically, we consider a source node which needs to offload data to a remote access point (AP) with which the source does not have a direct line-of-sight (LOS) channel, due to some blockage. For high-frequency channels, this blockage creates significant penetration loss, making direct communication with the AP costly in terms of energy consumption or potentially infeasible due to limits on transmit power. The source may try to enlist another nearby user equipment (UE) to act as an intermediate relay. However, to convince the non-cooperative entity to provide the relaying service, the source can use wireless power transfer (WPT) as a form of payment. Fig. 1 illustrates the problem scenario.

Our objective is to design a protocol which ensures that the source can communicate with the AP in an energy-efficient manner while accounting for the individual rationality of the participating entities. We approach the problem from a game-theoretic perspective and propose an auction-based protocol which achieves the desired system behavior. We next present a brief literature review before stating our contributions.

A. Literature Review

WPT involves the transfer of energy from one device to another without a wired connection, and while several technologies fall under the umbrella of WPT, we specifically consider RF-based WPT. In recent years, it has found many applications, from smart home ecosystems to industrial manufacturing [8]. For example, RF WPT can be used in Internet of Things (IoT) networks to charge batteries on small, remote devices, possibly with the aid of unmanned vehicles [9]. Experimental results demonstrate received powers in the microwatt or milliwatt ranges [10], and although comparatively inefficient compared to, e.g., inductive coupling, RF WPT can operate across greater distances (up to several km) [11]. Furthermore, as communication networks grow denser, harvesting ambient RF energy becomes a more attractive possibility, which has prompted research into hardware improvements [12, 13].

In the context of communication systems, the past several years have seen increased interest in simultaneous wireless information and power transfer (SWIPT), particularly in the context of IoT networks and cooperative relaying (CR) [14–19]. [14] considers a single BS using non-orthogonal multiple access (NOMA) to communicate with a near user and a far user while aided by a set of energy-harvesting relays. It then focuses on calculating the outage probability and finding the optimal power allocation while accounting for residual hardware errors and channel estimation errors. A SWIPT setup using antenna diversity receives attention in [15], which compares the performance of full-duplex to half-duplex relaying. The energy-harvesting relay node employs two batteries for greater efficiency, one for energy harvesting, the other to power the transmission. The outage probability and optimal power splitting ratios are found. In [16], the authors propose a wireless communication system integrating WPT and CR to enhance node operations and communication reliability. They explore both orthogonal and non-orthogonal CR schemes where multiple sources communicate with destinations via an energy-harvesting relay, adapting transmission strategies based on the relay decoding status. Numerical analysis demonstrates that the non-orthogonal CR scheme outperforms the orthogonal scheme in certain scenarios, influenced by parameters such as transmit powers, data rates, and terminal distances. [18] proposes a cooperative communication scheme based on WPT-enabled relaying that uses both time splitting (TS) and antenna switching (AS) paradigms, as well as self-energy recycling (SER). Splitting and switching ratios are optimized to maximize the communication rate, and the scheme is shown to outperform comparable designs. A comprehensive survey of WPT for CR is found in [19].

The aforementioned body of work focuses on cooperative settings, so that the source and the relay are generally analyzed or optimized as a single unit. In contrast, we consider a non-cooperative scenario, where other nodes must be incentivized to provide the relaying service. Such scenarios will naturally arise in next-generation communication networks, which will include many densely deployed UEs, from IoT devices, to wireless sensors, to autonomous vehicles, and personal devices such as smartwatches and phones [20, 21]. These devices, many of which will be battery-powered, may be owned by distinct entities, which are unlikely to expend their resources for the benefit of others. However, leveraging these devices for relaying could alleviate the need for deploying dedicated relays and would allow the communication topology to dynamically respond to real-time needs. For example, in a smart city deployment, IoT sensors or personal devices such as phones and wearables could opportunistically serve as relays to extend coverage in infrastructure-poor areas or reduce latency for time-sensitive applications, provided they are adequately incentivized. Thus, in this paper, we present a solution to the challenging problem of incentivizing non-cooperative UEs to perform a relaying service.

Many aspects of communication systems are well modeled as the interaction of non-cooperative, self-interested agents. Consequently, game theory and auctions have long been used to approach a wide range of problems, including resource allocation, relay selection, and power management [22–24]. For example, [24] uses a game-theoretic framework to develop a decentralized power allocation method which improves localization and energy efficiency in hybrid active-passive wireless sensor networks.

Several other works sit specifically at the intersection of WPT and game theory [25–30], including several that use non-cooperative games to understand how to manage interference, which, while detrimental to communication, may be harvested for additional energy [25, 26]. A Stackelberg game is deployed in [28] to analyze the behavior of end users serviced by a mobile UAV which provides both mobile edge computing (MEC) and energy transfer capabilities, and in [29], the Gale-Shapely matching algorithm is used to associate cluster heads, which act as energy harvesting relays, with clusters in a cognitive radio non-orthogonal multiple access system. In [30], a device-to-device caching system is studied, where some users cache popular content locally and are compensated via WPT by other users who utilize the cache. The system is analyzed as a Stackelberg game to characterize the interplay between the WPT payments and the caching policy.

Recent years have also seen the use of auctions and other market-based solutions to determine prices for WPT services. For example, [31] proposes a peer-to-peer double auction mechanism to extend the battery life of mobile devices. More recently, [32] considers the interaction between a network operator and a power supplier which uses WPT to charge network nodes. A Stackelberg game models their interaction, and the game framework enables price design for the WPT service while accounting for both the costs and battery efficiency in the network. The authors of [33] analyze pricing strategies for UAV-mounted chargers in wireless sensor networks using a Hotelling market model, while [34] extends this analysis to static UAVs in competitive markets. Both studies employ game-theoretic approaches to derive equilibrium pricing and maximize service provider profits. In [35], the authors consider a dynamic evolutionary game modeling an energy market, where several small-cell base stations buy and sell excess energy from each other. In these works, however, energy transfer is the objective rather than a means for incentivizing coordinated behavior, e.g., relaying.

Market-based solutions have also appeared in the context of WPT-enabled relaying. For example, in [27], a single relay serves multiple source-destination pairs and must decide how to allocate the power received from the sources for communication to the destinations. An auction-based approach is formulated to determine how to allocate the received power among the several destinations, and its Nash equilibria are studied. More recently, [36] proposes an auction-based method with payments in the form of virtual currency to select a relay node and transmit power in a multi-source sensor network. However, none of these works consider WPT itself as a form of payment.

While WPT and relay have appeared frequently in conjunction with auctions and other game-theoretical approaches, our work is unique in two fundamental ways. First, we use the auction to bring about WPT-enabled relaying in a non-cooperative setting. In this respect, our work is most similar to [27]. However in that paper, the auction determines how to allocate power which has already been harvested by a relay, while in our paper, the auction is used to select a suitable relay and determine the amount of energy to transfer via WPT. Second, we use energy itself as the medium of exchange. In this respect, our work bears some resemblance to [30], but we study WPT-based auctions for energy-efficient relaying, whereas [30] examines a Stackelberg game for the reduction of content delivery wait times in device-to-device caching.

In non-cooperative networks, designing an effective relaying protocol is challenging due to the self-interested nature of the UEs, which aim to maximize their utility by extracting as much energy from the source as possible. Additionally, the source lacks knowledge of the channel quality between UEs and the AP, complicating the selection of an efficient relay. Furthermore, the protocol must balance energy efficiency and communication reliability, while avoiding excessive computation or communication overhead, making the design of incentive-compatible protocols in non-cooperative settings a complex yet critical task.

To address these challenges, we propose protocols based on Vickrey [37] and Myerson [38] auctions. In a Vickrey auction (also known as a second-price, sealed-bid auction), the highest bidder wins but pays an amount equal to the second-highest bid. This mechanism is efficient in the sense that the item is always allocated to the participant who values it most. In contrast, a Myerson auction is a modified Vickrey auction in a Bayesian setting that maximizes the auctioneer's expected profit. However, this comes at the cost of occasional inefficiency, as the highest-value bidder may not always win. Importantly, both Vickrey and Myerson auctions are incentive-compatible, meaning that bidders are best off truthfully reporting their valuations [39]. In this paper, we leverage this property to design and analyze protocols based on these auctions, exploring the properties of Vickrey and Myerson auctions in the context of the WPT-enabled relay system. We next outline our contributions.

B. Contributions

This paper provides several contributions to the literature, as enumerated below:

- We present the problem of using WPT to induce energy-efficient relaying in a non-cooperative setting by modeling the battery-powered relaying candidates as rational, utility-maximizing agents that must be motivated to act as relays through a payment of energy. We propose the use of WPT-based auctions, implemented in a simple protocol, to achieve the coordination required for the relaying service in the non-cooperative setting, and for comparison, we also present a cooperative baseline.
- For Vickrey WPT auctions (VWAs), we mathematically prove that the outage probability is minimized, as is in the case of the cooperative baseline. We show that this outage probability decays exponentially as the number of candidates grows, and we mathematically characterize the energy efficiency gap compared to the cooperative baseline.
- As an alternative, we propose Myerson WPT auctions (MWAs), which significantly improve energy efficiency. We first rigorously develop a novel extension of the classical regularity result to reverse Myerson auctions, then mathematically prove the regularity of the MWA with both lognormal and Rayleigh fading. We then mathematically characterize the outage probability, and show that, although the outage probability increases compared to the VWA, the gap in outage probability decays exponentially as the number of candidates grows.
- Finally, we present several numerical studies that illustrate how system parameters (e.g., the number of candidates, the fading parameters, and the auction type) affect the outage probability, the source's energy consumption, and the energy harvested by the candidate. Comparing the results for the VWA and MWA, we offer insights into the tradeoffs of each auction type and give guidance when one auction type is preferred over the other.

Aspects of this work appear in our conference paper [40], which focuses on Myerson auctions with lognormal fading. As well as providing detailed proofs omitted from [40] due to space constraints, this paper analyzes Vickrey auctions and further examines the Myerson auction under a Rayleigh fading model. Furthermore, we provide an in-depth comparison of the Vickrey and Myerson auctions and give guidance on when one type of auction is preferred over the other.

The rest of the paper is organized as follows. In Section II, we lay out the communication and WPT models used throughout the paper, and in Section III, we present our auction-based protocol. We then analyze systems performance of the protocol when using a Vickrey auction in Section IV and when using a Myerson auction in Section V. Section VI then corroborates the analytical results and illustrates the impact of various system parameters, and Section VII concludes the paper.

II. System Modeling

We consider a system consisting of a source UE; a set of n battery powered UEs, referred to as candidates; and a single access point (AP). The source is located at $q_s \in \mathbb{R}^2$, and the candidates are located at positions $q_i \in \mathbb{R}^2, \forall i \in \mathcal{N}$, where $\mathcal{N} = \{1, \dots, n\}$. We treat q_i as independently distributed over the region of interest, $\mathcal{Q}$, and without loss of generality, we assume the access point is located at the origin. The system is illustrated in Fig. 2.

The source must transfer data to the AP in a timely manner. To do so, it may either try to send the data itself, or it may try to induce one of the candidates to provide a

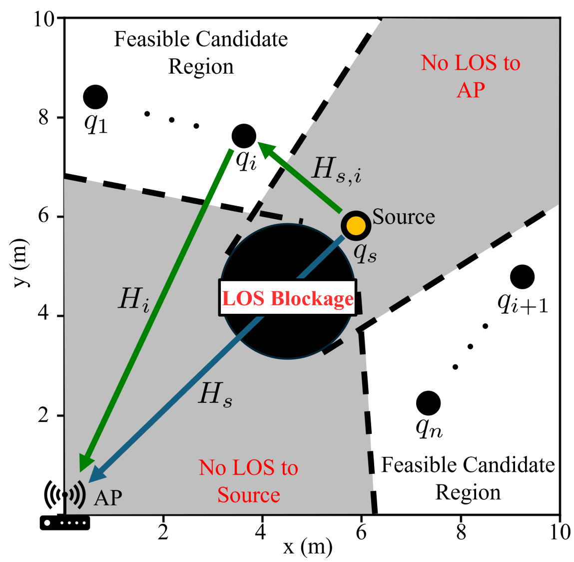

Fig. 2. System setup for the WPT-enabled relaying scenario. The orange dot gives the location of the source, q_s, the black dots give the locations of the candidates, q_i, and the AP is at the origin. The large black circle in the center indicates the blockage, and the gray region indicates the area where the channel to either the source or the AP is NLOS. The arrows represent channels, with the green arrows representing channels used if UE i acts as the relay. The channels are labeled with corresponding channel power variables.

relaying service using WPT energy payments. In the rest of this section, we provide our communication model, including channel modeling, as well as our model for WPT.

A. Channel Modeling and Communication

Let the source-to-AP, candidate-to-AP, and source-to-candidate wireless communication channel power (square of the modulus of the complex-valued channel gain) be denoted H_s, H_i, and $H_{s,i}$, respectively. We assume that these are sufficiently well-estimated by both the transmitter and receiver, so that the source knows H_s and $H_{s,i}$, $\forall i \in \mathcal{N}$, and the i^{th} candidate knows $H_{s,i}$ and H_i. However, the source and candidates do not know channel coefficients for channels which they do not use, so that the source does not know H_i, $\forall i \in \mathcal{N}$, and the i^{th} candidate does not know H_s and H_j, $\forall j \in \mathcal{N} \backslash i$. Thus, in auction terminology, the power of the candidate-to-AP channel, H_i, constitutes *private information*.

As in [40], we model each channel as composed of path loss and small-scale fading components, with large-scale shadowing modeled by using different parameters for LOS and non-LOS (NLOS) channels. More specifically, for $l \in \{s, i, si\}$ we have $H_l = H_{l,\text{PL}} H_{l,\text{f}}$, where $H_{l,\text{PL}}$ is the path loss component, and $H_{l,\text{f}}$ is the fading component, commonly modeled as a lognormal, Rayleigh, or Rician random variable [41]. The path loss component is modeled as $H_{l,\text{PL}} = K d_l^{-\eta}$, with K and η the path loss intercept and exponent, respectively, and d_l the distance between the transmitter and receiver. Path loss parameters K and η take on different values for the LOS and NLOS cases, and we distinguish these values with LOS and NLOS superscripts (e.g., K^{LOS}, K^{NLOS}). We will assume that H_s is a NLOS link, motivating the need to find a relay, and that H_i, $H_{s,i}$ are LOS links, as otherwise, candidate i would almost surely provide no advantage over the direct NLOS link.

To model channel capacity, we rely on the Shannon-Hartley theorem, so that the maximum achievable spectral efficiency over the channel is

$$r_{\max} = \log_2 \left(1 + P_{TX} H_l / \sigma^2\right), \tag{1}$$

where P_{TX}, H_l, and σ^2 are the transmit power, channel power, and receiver noise power, respectively. We further assume that the source and all UEs have a maximum transmit power $P_{\max}$. Consequently, for transmission with spectral efficiency r to be successful, we must have $r \leq \log_2 \left(1 + P_{\max} H_l / \sigma^2\right)$.

B. Data Transfer Requirements

The source must transfer a given amount of data to the destination within a fixed amount of time, T. This models scenarios with hard time-related constraints, such as vehicular systems (V2X), AR/VR, or industrial automation. We do not assume that satisfying the time constraint is always feasible, and thus we examine system performance in terms of both energy consumption and outage probability. We note that using the maximum allowed time, T, results in the lowest energy usage [42], so that, without loss of generality, we will assume the full time T is always used for the relay procedure[1].

Let D represent the bandwidth-normalized amount of data (in bit/Hz) that must be transferred. The specification of both T and D induces a spectral efficiency requirement of $r > D/T$ (bit/s)/Hz, so that for the source to transfer the data directly to the AP, its minimal transmit power is $P_s = \zeta / H_s$, where $\zeta = (2^{D/T} - 1)\sigma^2$ is the minimum required received power to communicate at a rate of D/T. For deep fades (poor channel conditions) or short transmit times, this value may be quite large, and may in fact exceed $P_{\max}$. Alternatively, the source may use WPT to incentivize a candidate to act as a decode-and-forward relay to the AP.

C. Relaying and WPT

Relaying data to the AP via one of the candidates requires two transmissions, and we assume that, due to either the use of orthogonal frequency bands or full-duplex relaying capabilities, additional delay due to the relaying operation is negligible. First, to transmit the data to the candidate, the source must transmit with a power of at least $P_{s,i} = \zeta / H_{s,i}$. Then, the candidate must transmit the data to the AP with a power of at least $P_i = \zeta / H_i$. To incentivize the candidate, however, the source must also send enough energy to the candidate to at least cover the cost of transmission. Let P_{WPT} be the power allocated for wireless power transfer. The power harvested by the i^{th} UE, $P_{\text{harv},i}$, depends on a number of factors, including the channel between the source and the candidate, $H_{s,i}$, the effective aperture of the receiver antenna, A_r, and the energy-harvesting circuitry efficiency, α [17]. Formally, we have $P_{\text{harv},i} = P_{\text{WPT}} H_{s,i} A_r \alpha = \tilde{\alpha}_i P_{\text{WPT}}$ where $\tilde{\alpha}_i = H_{s,i} A_r \alpha$ is the overall efficiency of the WPT.

We consider simultaneous wireless information and power transfer (SWIPT), in which WPT and communication happen concurrently, implemented with power-splitting [43], so that

[1]This assumption can also be explicitly derived within a multi-attribute auction framework, but this requires substantial additional notation and ultimately simplifies to the formulation we consider.

q_s	Source position	q_i	i^{th} candidate position	ζ	Min. required received power
σ^2	Receiver noise power	H_s	Channel power, source to AP	H_i	Channel power, candidate i to AP
$H_{s,i}$	Channel power, source to candidate i	P_{tot}	Total source transmit power	$P_{\max}$	Max. transmit power
D	Bandwidth-normalized data requirement	T	Maximum transmit time	$\tilde{\alpha}_i$	Overall WPT efficiency for candidate i
P_s	Min. TX power, source to AP	$P_{s,i}$	Min. TX power, source to candidate i	P_i	Min. TX power, candidate i to AP

TABLE I
IMPORTANT SYSTEM VARIABLES

if the source chooses candidate i as the relay, its total power consumption is $P_{\text{tot}} = P_{s,i} + P_{\text{WPT}}$, with $P_{s,i}/P_{\text{tot}}$ the receiver's power splitting ratio. **The key question addressed in this paper is this: how can the source determine which candidate to use (if any) and total transmit power, P_{tot}, in this non-cooperative setting?**

III. An Auction Formulation

We view the source and all candidates as rational decision makers seeking to non-cooperatively maximize their individual utilities. The source and the candidates both seek to minimize their net energy expenditure. Additionally, the source must ensure that the data is offloaded within the time limit, T. These preferences are captured in the following utility functions for the source and candidates, denoted as U_s and U_i, respectively:

$$U_s = Cz - TP_{\text{tot}},$$
$$U_i = \begin{cases} 0 & \text{If } \rho \neq i \\ a_i T(\tilde{\alpha}_i(P_{\text{tot}} - P_{s,i}) - P_i) & \text{If } \rho = i \end{cases}, \tag{2}$$

where C is a large reward modeling successful data transmission to the AP within the time budget, $z \in \{0, 1\}$ indicates whether this is actually achieved, ρ is the index of the candidate chosen for relaying (if any), and $a_i \in \{0, 1\}$ indicates whether a chosen candidate agrees to take on the relaying service. To enforce the rationality of the candidates, we have

$$a_i = \begin{cases} 1 & \text{if } \tilde{\alpha}_i(P_{\text{tot}} - P_{s,i}) - P_i \geq 0 \\ 0 & \text{Otherwise} \end{cases},$$

so that the candidate only agrees to take on the relaying task if the will not result in a net loss of energy. Note that when $\tilde{\alpha}_i(P_{\text{tot}} - P_{s,i}) - P_i = 0$, the candidate is indifferent between accepting and rejecting the agreement, and for ease of exposition, we assume that in this case the candidate will accept[2]. For the source, smaller values of C emphasize energy efficiency, while larger values of C place greater weight on ensuring successful communication, and to ensure that the source always has positive utility when communication is successful, we have $C > TP_{\max}$. Finally, we also assume that the transmission is sufficiently spatially constrained so that if a candidate is not chosen as the relay, it cannot harvest energy, though relaxing this assumption is an important direction for future work.

A reverse auction, sometimes called a procurement auction, naturally frames the considered scenario. In this framework, the source looks to "buy" relaying services from the candidates, who bid for the opportunity to provide the service. In practice, the communication protocol proceeds as follows: (1) The source broadcasts a request for bids; (2) The candidates respond with bids; (3) the source broadcasts its choice of the winner, ρ, as well as the price, P_{tot}; (4) the winner accepts or rejects; (5) the relaying process begins. This process disallows extended bargaining between the source and candidates, which is desirable given the potential costs in both time and energy that could result. For ease of exposition, we consider bids as proposed values of the total source transmit power, P_{tot}. This is equivalent to bids in terms of total source energy usage, TP_{tot}, since the source will always use the full time to transmit. Furthermore, since both the source and candidate know the value of $H_{s,i}$, this is equivalent to expressing bids as proposed values of P_{WPT}. We next present details of the auction-based protocol.

A. Auction Components

We next review the components of an auction and their corresponding concepts in our WPT-enabled relaying setting.

Valuations: In a reverse auction, the valuations, $\mathcal{V} = \{v_0, ..., v_n\}$ indicate how much the service is worth to the participants, where v_0 is the value of the service to the procurer, and v_i, $\forall i \in \mathcal{N}$ is the cost that would be incurred by the bidders if they had to provide the service.

Thus, the valuation of the source (the service procurer) is the power required to directly transmit the data to the AP. Recall that P_s is the minimum power required for direct transmission to the AP. If $P_s < P_{\max}$, then $v_0 = P_s$. However, if $P_s \geq P_{\max}$ the source cannot transmit the data directly within the time frame. In this case, we set $v_0 = P_{\max}$, with the interpretation that this is the maximum power the source could possibly use for WPT payment. Consequently, $v_0 \leq P_{\max}$ always holds.

The valuations of the candidates may be similarly modeled. If the source elects to send data via the i^{th} candidate, it must transmit with a power of at least $P_{s,i} + P_i/\tilde{\alpha}_i$, which ensures non-negative utility for the i^{th} candidate. Thus, $v_i = P_{s,i} + P_i/\tilde{\alpha}_i$. Note that, to facilitate comparison, the valuation is expressed in terms of the power required by the source, not the power used by the candidate. Importantly, there is a one-to-one mapping between v_i and the private information H_i, so that bidding v_i is equivalent to revealing H_i.

Bids: The candidates' valuations depend on private channel information, H_i, which is not known by the source. Thus, in a general setting, the candidates could provide bids that differ from their true valuations, as their goal is to maximize their profit. However, this paper considers two specific auction rules (*mechanisms*) under which bidding the true valuation maximizes a candidate's utility. These *incentive-compatible* mechanisms have been well-studied in game theory literature and applied across a variety of domains [39]. As we discuss in greater detail later in this section, using a mechanism that results in the candidates' biding their true valuations differs in subtle but important ways form assuming that the source

[2]We assume candidates are not malicious, meaning they will honor their commitment if they agree to relay.

knows all the valuations beforehand or that the candidates act cooperatively with the source.

Mechanisms: A mechanism is defined by two functions, $\rho(\mathcal{V})$ and $X(\mathcal{V})$, which take as arguments the set of valuations, $\mathcal{V}$, and determine the winner of the auction and the payment to the winner, respectively. In the context of the WPT scenario, $\rho(\mathcal{V})$ indicates which of the candidates will act as the relay, and $X(\mathcal{V})$ gives P_{tot}. Note that $\rho(\mathcal{V}) = 0$ indicates the source will not try to relay through any of the candidates. If that is the case and $P_s \leq P_{\max}$, the source successfully sends the data directly. Otherwise, a communication outage occurs, and we assume that the source, knowing that the transmission will be unsuccessful, uses $P_{\text{tot}} = 0$. More generally, it will not transmit at all if communication cannot occur within the given time frame through any of the candidates or itself.

B. System Metrics

The trade-off between communication reliability and energy efficiency constitutes a fundamental challenge in our communication system, and we consider the outage probability and energy consumption as the core performance metrics of our proposed protocol. We next discuss each of these in more detail.

1) Outage Probability: An outage occurs when the source is unable to transfer data to the AP, which corresponds to $z = 0$. For a given mechanism and a set of valuations, we have

$$z = \begin{cases} 1 & \text{If } \rho(\mathcal{V}) \neq 0 \text{ and } X(\mathcal{V}) \geq v_{\rho(\mathcal{V})} \\ 1 & \text{If } \rho(\mathcal{V}) = 0 \text{ and } P_s \leq P_{\max} \\ 0 & \text{Otherwise.} \end{cases} \quad (3)$$

For a given mechanism, the outage probability is the probability that the mechanism does not successfully transfer the data within the time limit, T, and we define this probability in the *ex-ante* sense, i.e., considering uncertainty both in the candidate placement and fading realization. Thus, for a set of n relay candidates, we formally define the outage probability as follows:

$$P_{\text{out}} = \int_{\mathcal{V}\in\mathcal{S}_\mathcal{V}} \delta\left(1 - z\left(\rho(\mathcal{V}), X(\mathcal{V})\right)\right) f_{\mathcal{S}_\mathcal{V}}(\mathcal{V}) d\mathcal{V}, \quad (4)$$

where $S_\mathcal{V}$ is the set of all sets of valuations, and where $\delta(l) = 1$ if $l = 0$ and $\delta(l) = 0$ otherwise. The PDF $f_{\mathcal{S}_\mathcal{V}}(\mathcal{V})$ gives the likelihood of a specific valuation set, $\mathcal{V}$, which depends on the distribution of fading on each channel as well as the placement of each of the relay candidates, which will be given in more detail latter in the context of specific fading models.

An outage may happen either because there is no feasible route for communication, i.e., $P_s > P_{\max}$ and $v_i > P_{\max}$, $\forall i \in \mathcal{N}$, or due to the auction mechanism itself. This leads to the following definition:

Definition 1. *A mechanism is said to* ***minimize the outage probability*** *if an outage occurs only when the quality of communication channels precludes data offloading, via any of the candidates or via the source itself, within the time frame, T. Formally, this is expressed as $((\rho(\mathcal{V}) = 0) \wedge (P_s > P_{max})) \implies (\min_{i\in\mathcal{N}} v_i > P_{max})$. The corresponding* ***minimum outage probability*** *is denoted as p^*_{out}.*

Importantly, when using a mechanism that minimizes the outage probability, communication occurs whenever feasible.

2) Energy Consumption: To evaluate energy use in the system, we consider the sum of the net energy consumption of each node. The source uses energy TP_{tot}, and if there is a winning candidate, it uses energy TP_ρ, where the dependence of ρ on $\mathcal{V}$ has been dropped for readability in the subscript. Additionally, a winning candidate harvests energy $T\tilde{\alpha}_\rho P_{\text{tot}}$, so the net energy consumed in the system is $T(P_{\text{tot}}+P_\rho-\tilde{\alpha}_\rho P_{\text{tot}}) = T(P_{\text{tot}} - \Delta P_\rho)$, where $T\Delta P_\rho = T(\tilde{\alpha}_\rho P_{\text{tot}} - P_\rho)$ is the net energy gain of a winning candidate. However, practical experiments documented in the [10] and references therein indicate that that the net power harvested by a winning candidate will be orders of magnitude smaller than the total transmit power of the source. Thus, when discussing energy efficiency, we focus on the source's energy consumption. In our analysis presented in Sections IV and V, we discuss energy consumption in the *ex-post* sense, i.e., considering the final outcome of the protocol for specific realizations of candidate placement and channel fading. In Section VI, numerical results show energy consumption in the *ex-ante* sense, i.e., as expected or average values.

C. A Cooperative Lower Bound

To provide a best-case performance bound for comparison, we briefly consider the scenario where the candidates work cooperatively with the source, i.e., where $U_i = U_s = Cz - TP_{\text{tot}} + \sum_{i\in\mathcal{N}} \Delta\epsilon_i$, where $\Delta\epsilon_i$ is the net energy change of a relay candidate as given in (2). In this scenario, the source and the UEs work together to minimize the total system energy consumption while also ensuring that communication is achieved ($z = 1$), if possible. To respect the energy constraints of the relay candidates, (3) still holds, that is, the chosen relay candidate must still harvest at least as much energy as it expends while performing the relay service.

Although we consider the cooperative scenario, the relay candidates still hold private information, v_i, which the source must obtain using the protocol described earlier. The source first broadcasts a request for information, the relay candidates respond with v_i, and finally the source makes a decision based on the given information. In particular, we have

$$\begin{aligned} \rho^C(\mathcal{V}) &= i^* = \underset{i\in\mathcal{N}\cup\{0\}}{\arg\min}\, v_i \\ X^C(\mathcal{V}) &= v_{i^*} \end{aligned} \quad (5)$$

Note that this mechanism satisfies the condition given in Definition 1 and thus achieves the minimum outage probability. Furthermore, X^C clearly gives the least amount of energy the source can use to successfully communicate with the AP, and it can easily be shown that in the most energy efficient system, no excess energy is harvested by a chosen relay candidate, due to the losses incurred by WPT (i.e., the fact that $\tilde{\alpha} < 1$). Thus, the protocol also minimize the total system energy consumption.

For both the cooperative and non-cooperative scenarios considered in the paper, the relay candidates report their true valuations, v_i. However, in the former case it is due to a shared objective while in the latter case, it is due to the incentive compatibility of the mechanism. To illustrate, note that if the mechanism in (5) were employed in a non-cooperative scenario, we would have a classical first-price sealed-bid auction, which is not incentive compatible [39]. More specifically, non-cooperative relay candidates would tend to submit bids higher than their true valuations, and the source would end up using more energy than in the cooperative case.

Remark - The Role of Private Information An alternative view of the problem is that the lack of information on H_i leads to the difference in outcomes between the cooperative and non-cooperative scenarios. If the source knows H_i, $\forall i \in \mathcal{N}$ beforehand in the non-cooperative case, it can make a take-it-or-leave-it offer to the best candidate, which the candidate would accept since it still has non-negative utility. This outcome would be identical to the outcome of the cooperative mechanism given in (5). However, the private information held by the relay candidates precludes this outcome.

We next evaluate the system under a Vickrey-auction-based protocol. As we shall see, the lack of cooperation and information leads to some performance loss, but as the number of candidates increases, the results of the auction approach those of the cooperative baseline, as verified in Section VI.

IV. Vickrey WPT Auctions (VWA)

This section considers system performance when the protocol described in Section III employs a Vickrey auction, and we refer to this protocol as the Vickrey WPT Auction (VWA). We first present the Vickrey mechanism, then analyze the outage probability, mathematically characterizing it as a function of the number of candidates. Finally, we discuss energy consumption, which motivates the Myerson mechanism introduced in Section V.

A. The Vickrey Mechanism

The standard Vickrey auction [37] is a classical incentive-compatible mechanism. For a reverse auction, it is defined as:

$$\begin{aligned} \rho^{\mathrm{V}}(\mathcal{V}) &= i^* = \arg\min_{i \in \mathcal{N} \cup \{0\}} v_i \\ X^{\mathrm{V}}(\mathcal{V}) &= \begin{cases} v_{\hat{i}} & \text{If } \rho^V(\mathcal{V}) \neq 0 \\ v_0 & \text{If } \rho^V(\mathcal{V}) = v_{i^*} \end{cases}, \end{aligned} \tag{6}$$

where $\hat{i} = \arg\min_{i \in \mathcal{N} \cup \{0\} \setminus i^*} v_i$ In words, the participant, either candidate or source, with the lowest valuation wins[3]. If the winner is a candidate, then the source pays the amount of the second-lowest valuation, while if the winner is the source itself, it "pays" itself its own valuation (no transfer is made).

B. Outage Probability

Recall from Section III that if data transfer is not complete within the time frame T, we say an outage has occurred, and let p^V_{out} denote the outage probability under the VWA. We now prove that the VWA minimizes the outage probability (Definition 1) before mathematically characterizing this minimum outage probability.

[3]Valuations are dependent on communication channel powers, which are continuous random variables, so that we will almost surely never have two valuations equal to each other, and we omit tie-breaking rules for brevity.

Lemma 1. *The VWA minimizes the outage probability, as described in Definition 1.*

Proof. Recall that if $P_s > P_{\max}$, we have $v_0 = P_{\max}$, and suppose that $P_s > P_{\max}$ and $\rho^V(\mathcal{V}) = 0$. By the definition of $\rho^V(\mathcal{V})$in Eq. (6), this implies $v_0 = P_{\max} < \min_{i \in \mathcal{N}} v_i$, which satisfies the condition stated in Definition 1.

As a consequence of Lemma 1, we have $p^V_{\text{out}} = p^*_{\text{out}}$, and the VWA achieves the same outage probability as the cooperative baseline. We next mathematically characterize this minimum outage probability.

From the discussion of the valuations in Section III, we see that an outage occurs if and only if $\min_i v_i > P_{\max}$ and $P_s > P_{\max}$. For the source, this implies $P_{\max} < \zeta/H_s$, while for each individual candidate, we must have $P_{\max} < \zeta(1/(\alpha A_r H_{s,i} H_i) + 1/H_{s,i})$. Recall from Section II that $H_l = H_{l,\text{PL}} H_{l,\text{f}}$ for $l \in \{s, i, si\}$, where the path loss component $H_{l,\text{PL}}$ is determined by the distance between the two nodes on the link. Let $F_{H^{\text{NLOS}}_{\text{f}}}(h_{\text{f}})$ denote the CDF of the fading in the NLOS case. For a given source location q_s, we can then calculate the outage probability at the source as follows:

$$p_{\text{out},s} = \Pr\left(P_{\max} < \zeta/H_s\right) = F_{H^{\text{NLOS}}_{\text{f}}}\left(\zeta/(H_{s,\text{PL}} P_{\max})\right). \tag{7}$$

We model the event that the individual candidates experience an outage, i.e., cannot feasibly act as relays, as independently and identically distributed (i.i.d.). To see this, first note that channel measurement campaigns indicate that in low-scattering environments, small-scale fading spatially decorrelates within a few wavelengths [41], while for scattering rich-environments, decorrelation can occur within a half a wavelength, as in the classical Jakes model [44]. For a transmission at 5GHz, this translates to decorrelation in 3 to 12 cm, while for higher frequencies, decorrelation can occur within a centimeter or less. We therefore treat fading as independent across channels. We also model the candidates' placements as independent, so that the path loss components of the channel powers are independent as well.

Let H_c and $H_{s,c}$ denote the candidate-to-AP and the source-to-candidate channel power, respectively, for an arbitrary candidate. Further, let $f_Q(q)$ denote the PDF of the spatial distribution of the generic candidate, and let $f_{H^{\text{LOS}}_{\text{f}}}(h_{\text{f}})$ and $F_{H^{\text{LOS}}_{\text{f}}}(h_{\text{f}})$ denote the PDF and CDF of the LOS fading, respectively. Then integrating over possible candidate placements and channels realizations, we calculate the outage probability for an arbitrary candidate as:

$$\begin{aligned} p_{\text{out,c}} &= \Pr\left(P_{\max} < \zeta(1/(\alpha A_r H_{s,c} H_c) + 1/H_{s,c})\right) \\ &= \int_{q \in Q} f_Q(q) \int_{h=0}^{\infty} f_{H^{\text{LOS}}_{\text{f}}}(h) F_{H^{\text{LOS}}_{\text{f}}}\left(g(q,h)\right) dh dq, \end{aligned} \tag{8}$$

where Q is the region in space such that the point $q \in Q$ has a LOS channel to both the AP and source, and where

$$g(q,h) = \frac{1}{\zeta}\left(\frac{P_{\max}}{\alpha A_r H_{s,i,\text{PL}}(q) H_{i,\text{PL}}(q) h} + \frac{P_{\max}}{H_{s,c,\text{PL}}(q)}\right)^{-1}.$$

Here, $H_{c,\text{PL}}(q) = K^{\text{LOS}} ||q||_2^{-\eta^{\text{LOS}}}$ and $H_{s,c,\text{PL}}(q) = K^{\text{LOS}} ||q - q_s||_2^{-\eta^{\text{LOS}}}$ are the path loss component of the candidate-to-AP and source-to-candidate channels, respectively, given the candidate location, q. The overall outage probability is then given by:

$$p^*_{\text{out}} = p^V_{\text{out}} = p_{\text{out},s}\, p_{\text{out,c}}{}^n. \tag{9}$$

The above expression shows that the outage probability decays exponentially as the number of candidates increases, with the base, $p_{\text{out,c}}$, dependent on the spatial distribution of the candidates, among other factors. **In summary, we have shown that the VWA minimizes the outage probability (see Definition 1), we have mathematically characterized this minimum outage probability, and we have shown that the outage probability decays exponentially as the number of candidates increases.**

C. Energy Consumption

We next evaluate the system-wide energy consumption, assuming that communication is possible. If $i^* = 0$, then the energy consumption is simply $Tv_{i^*} = Tv_0 = TP_s$. Importantly, the energy consumption in this case is identical for the cooperative baseline and the VWA. When $i^* \neq 0$, however, the VWA results in additional energy usage. The total energy consumption is given by $Tv_{\hat{i}} - T\tilde{\alpha}_{i^*}(v_{\hat{i}} - v_{i^*})$, where the first term captures the source's energy consumption, and the second term accounts for the net energy harvested by the candidate. Comparing with the cooperative baseline, for which the energy consumption is given by Tv_{i^*}, the difference in energy is

$$\Delta\mathcal{E} = (1 - \tilde{\alpha}_{i^*})T(v_{\hat{i}} - v_{i^*}).$$

The above expression accounts for the fact that the source uses $(v_{\hat{i}} - v_{i^*})$ more power, which is only slightly offset by the net $\tilde{\alpha}_{i^*}(v_{\hat{i}} - v_{i^*})$ power harvested at the relay, since in general $\tilde{\alpha}_{i^*}$ is orders of magnitude less than 1. **Thus, the VWA is less energy efficient than the cooperative baseline.**

The expression above indicates two approaches for improving energy efficiency. First, improving WPT efficiency $\tilde{\alpha}_i$ through, e.g., hardware improvements, reduces the cost of energy transfer. Second, reducing the gap between $v_{\hat{i}}$ and v_{i^*} will also bring the performance of the VWA more closely in line with cooperative baseline. This could be achieved by increasing the number of candidates, as illustrated in Section VI. Alternatively, the source may employ a different type of auction which, on average, brings its total TX power, $X(\mathcal{V}) = P_{\text{tot}}$, closer to the minimum, v_{i^*}, while maintaining incentive compatibility. This possibility is explored next.

V. Myerson WPT Auctions (MWA)

In this section, we consider an alternative protocol based on a Myerson auction, which reduces the source's energy usage, and we refer to this protocol as the Myerson WPT Auction (MWA). Myerson auctions [38] are known to maximize the auctioneer's utility, so that on average, they will minimize the source's energy consumption. These auctions are defined within a Bayesian setting, so the source must know the probability distribution from which the candidates' valuations are drawn. For the MWA, this amounts to knowing the distributions over H_i, $\forall i \in \mathcal{N}$. With this additional information, it's possible to construct a mechanism that, on average, improves the energy efficiency of the system.

The general Myerson mechanism can be computationally cumbersome, but when a set of regularity conditions are met, the mechanism becomes easily computable. In the rest of the section, **we first extend classical results on regular Myerson auctions to the reverse auction setting and prove the regularity of the MWA for lognormal and Rayleigh fading. We then mathematically characterize the outage probability and show the improved energy efficiency.**

A. Reverse Myerson Auctions

In this section, we develop a novel extension of results for Myerson auctions. Myerson auctions resemble Vickrey auctions, but rather than comparing valuations directly, *virtual valuations* are used to determine the winner and payment. In general, determination of virtual valuations requires a potentially complex "ironing" procedure [38]. However, if the distributions over the valuation satisfy a regularity condition, the mechanism simplifies greatly. After first presenting this established regularity condition and associated mechanism for forward auctions, we extend the Myerson framework by mathematically proving the equivalent regularity condition and mechanism for reverse auctions.

Let $F_{V_i}(v_i)$ and $f_{V_i}(v_i)$ denote the CDF and PDF, respectively, of a generic valuation, v_i, with support Θ_i. We now present the standard regularity definition.

Definition 2. *(Forward Regularity) Let $c^f_i(v_i) = v_i - \frac{1-F_{V_i}(v_i)}{f_{V_i}(v_i)}$. A forward Myerson auction is **regular** if $dc^f_i(v_i)/dv_i \geq 0, \forall v_i \in \Theta_i, \forall i \in \mathcal{N}$. Furthermore, $c^f_i(v_i)$ is the **forward auction virtual valuation**.*

Note that the virtual valuations are defined only for the bidders. However, for ease of notation, we define $c^f_0(v_0) = v_0$. We may now restate Myerson's result:

Theorem 1. *For regular forward Myerson auctions, the seller-optimal mechanism is given by:*

$$\begin{aligned} \rho^{f,M}(\mathcal{V}) &= \max_i \left\{c^f_i(v_i)\right\}^n_{0=1} \\ X^{f,M}(\mathcal{V}) &= \begin{cases} \omega^{f,M} & \text{If } \rho^{f,M}(\mathcal{V}) \neq 0 \\ 0 & \text{If } \rho^{f,M}(\mathcal{V}) = 0 \end{cases} \end{aligned} \tag{10}$$

with $\omega^{f,M} = \inf\left\{s | c^f_{\rho^{f,M}}(s) > \max\{c^f_i(v_i)\}^n_{i=0}\right\}$.

Proof. See [38].

Thus, the winner of the forward auction is the bidder with the highest *virtual* valuation, and their payment corresponds to the virtual valuation of the second-highest bidder. The above result holds for forward auctions, but our WPT-enabled relaying scenario is best modeled as a reverse auction, as the bidders are offering to provide a service at a cost. We next extend this result to the reverse auction:

Definition 3. *(Reverse Regularity) Let $c_i(v_i) = v_i + \frac{F_{V_i}(v_i)}{f_{V_i}(v_i)}$. A reverse Myerson auction is **regular** if $dc_i(v_i)/dv_i \geq 0, \forall v_i \in \Theta_i, \forall i \in \mathcal{N}$ Furthermore, c_i is the **reverse auction virtual valuation**.*

For ease of notation, we again set $c_0(v_0) = v_0$, and we now extend Theorem 1.

Corollary 1. *For a regular reverse Myerson auction the buyer-optimal mechanism for reverse auctions is given by:*

$$\rho^M(\mathcal{V}) = \min_i \quad \{c_i(v_i)\}_{i=0}^n$$
$$X^M(\mathcal{V}) = \begin{cases} \omega^M & \text{If } \rho^M(\mathcal{V}) \neq 0 \\ 0 & \text{If } \rho^M(\mathcal{V}) = 0 \end{cases}, \tag{11}$$

with $\omega^M = \sup\left\{s | c_{\rho^M}(s) < \min\left\{c_i(v_i)\right\}_{i=0}^n\right\}$.

Proof. See Appendix A.

By proving the Myerson regularity condition and mechanism structure for reverse auctions, we have derived conditions under which the Myerson pricing mechanism is easily implementable. We next show that under lognormal fading and Rayleigh fading, the MWA satisfies the reverse regularity condition in Definition 3.

B. Regularity of WPT Auctions

We now show the regularity of the MWA under lognormal and Rayleigh fading. For tractable analysis, we assume that the source has partial information about the candidate-to-AP downlink channel power, H_i. Specifically, we assume the locations of the candidates and path loss parameters are available to the source, so that the path loss component of the channel, $H_{i,\text{PL}}$, is known. We also assume that the parameters needed to model fading, specified below, are known[4]. However, the fading realizations, $H_{i,\text{f}}$, $\forall i \in \mathcal{N}$ are unknown, and they are treated as i.i.d random variables with a known PDF and CDF of $f_{H_f^{\text{LOS}}}(h)$ and $F_{H_f^{\text{LOS}}}(h)$, respectively.

To simplify analysis, recall that $v_i = P_i/\tilde{\alpha}_i + P_{s,i}$, $\forall i \in \mathcal{N}$. Given our information assumptions, $P_{s,i}$ is constant while P_i is a random variable due to its dependence on the unknown fading power $H_{i,\text{f}}$. Letting $\tilde{v}_i = P_i/\tilde{\alpha}_i = C_i/H_{i,\text{f}}$, with $C_i = \zeta/(H_{i,\text{PL}}\tilde{\alpha}_i)$, we have $f_{V_i}(v_i) = f_{\tilde{V}_i}\left(v_i - P_{s,i}\right)$. Further, let $\tilde{c}_i(\tilde{v}_i) = \tilde{v}_i + F_{\tilde{V}_i}(\tilde{v}_i)/f_{\tilde{V}_i}(\tilde{v}_i)$, and note that $d\tilde{c}_i(\tilde{v}_i)/d\tilde{v}_i = dc_i(v_i)/dv_i$. Thus, we may equivalently show that the auction with valuations $\tilde{v}_i$ is regular. We now derive the cumulative distribution function of $\tilde{v}_i$:

$$\begin{aligned} F_{\tilde{V}_i}(\tilde{v}_i) &= \Pr\left(\tilde{V}_i \leq \tilde{v}_i\right) = \Pr\left(\frac{C_i}{H_{i,\text{f}}} \leq \tilde{v}_i\right) \\ &= 1 - \Pr\left(H_{i,\text{f}} \leq C_i/\tilde{v}_i\right) = 1 - F_{H_f^{\text{LOS}}}\left(h_i(\tilde{v}_i)\right), \end{aligned} \tag{12}$$

where $h_i(\tilde{v}_i) = C_i/\tilde{v}_i$. Noting that $h_i(\tilde{v})$ is monotonic in $\tilde{v}$, the PDF is given by $f_{\tilde{v}_i}(\tilde{v}_i) = f_{H_f^{\text{LOS}}}\left(h_i(\tilde{v}_i)\right) C_i/\tilde{v}_i^2$. We are now ready to develop the main results.

Lognormal fading: We first consider the case where fading power is modeled as a lognormal random variable. Discussion of lognormal fading generally characterize channel power in the dB domain, i.e., $H_{i,\text{f}}^{\text{dB}} = 10\log_{10} H_{i,\text{f}}$. For the derivations below, it will be more convenient to work with linear power, so that if $H_{i,\text{f}} \sim \text{Lognormal}(0, \sigma_f^2)$, then $H_{i,\text{f}}^{\text{dB}} \sim N(0, (10\sigma_f/\ln(10))^2)$, where N denotes the normal distribution.

[4]Candidate locations may be found using, e.g., integrated sensing and communication techniques [45]. The LOS channel path loss and fading parameters may be estimated from the source's interaction with the candidates over the source-to-candidate channel, which is also LOS.

Theorem 2. *Suppose that for all* $i \in \mathcal{N}$*, the fading is i.i.d with* $H_{i,f} \sim Lognormal(0, \sigma_f^2)$*. Then the WPT reverse Myerson auction is regular.*

Proof. See Appendix B.

The above result shows that under lognormal fading, the mechanism described in (11) minimizes the source's expected energy consumption. Furthermore, as a consequence of the monotonicity of $c_i(v_i)$ implied by regularity, the optimal transmit power $X^M(\mathcal{V})$ can be found with logarithmic time complexity using a simple bisection method.

Rayleigh fading: Rayleigh fading is another common fading model found in the literature. Importantly, Rayleigh fading refers to the distribution of the channel gain, the square root of the power, and if the channel gain is Rayleigh distributed with distribution parameter ψ_f, the channel power is exponentially distributed with average power $2\psi_f^2$ [44]. We now prove the regularity of the auction assuming this model.

Theorem 3. *Suppose that for all* $i \in \mathcal{N}$*, the fading is i.i.d with* $H_{i,f} \sim Exp(1/(2\psi_f^2))$*. Then the WPT reverse Myerson auction is regular.*

Proof. From Eq. (12) and the properties of the exponential distribution, we have

$$F_{\tilde{V}_i}(\tilde{v}_i) = 1 - (1 - e^{-h_i(\tilde{v}_i)/(2\psi_\text{f}^2)}) = \exp\left(\frac{-C_i}{2\tilde{v}_i\psi_\text{f}^2}\right)$$
$$f_{\tilde{V}}(\tilde{v}_i) = \frac{C_i}{2\tilde{v}_i^2\psi_\text{f}^2}\exp\left(\frac{-C_i}{2\tilde{v}_i\psi_\text{f}^2}\right).$$

We can now write $\tilde{c}_i(\tilde{v}_i) = \tilde{v}_i + 2\tilde{v}_i^2\psi_\text{f}^2/C_i$, which is monotonically increasing in $\tilde{v}_i$ for all $\tilde{v}_i \geq 0$.

The result presented above indicates that, with Rayleigh fading, the mechanism given in (11) minimizes the source's average energy usage. We note that the expression $\tilde{c}_i(\tilde{v}_i)$ is quadratic, so that finding the payment, $X^M(\mathcal{V})$, using the Myerson mechanism can be done in constant time.

Remark - Rician Fading: In addition to lognormal and Rayleigh fading, Rician fading is another important fading model found in the literature. Although Rayleigh fading can be seen as a Rician fading with a K-factor of 0 [44], **it is easy to produce counterexamples that illustrate that a general Rician distribution is not regular**, and thus more complex "ironing" techniques are needed for auctions in these scenarios [38]. Specifically, the ironing technique must determine the convex hull of the virtual valuation function, $c_i(v_i)$, which depends on non-analytic functions that appear in the PDF and CDF of the Rician distribution (an order-zero modified Bessel function of the first kind and a first-order Marcum Q-function, respectively). This presents a significant challenge in the derivation of a closed-form expression, and numerical methods would incur high computational costs and corresponding energy usage. This makes Myerson auctions under Rician fading more challenging compared to lognormal and Rayleigh fading, and we discuss this point further in Section VII.

C. Outage Probability

While the MWA promises greater energy efficiency on average compared to the VWA, it does not minimize the outage probability. To illustrate, consider a simple scenario consisting of a single candidate and the source, with $P_s > P_{\max}$ and $v_1 < P_{\max} = v_0 < c_1(v_1)$. The VWA results in the candidate winning and the source using total power $P_{\max}$. However, for the MWA, the source wins but cannot communicate. Thus, while the MWA requires less energy on average, it does so at the cost of increased outage probability. We next characterize the extent to which the MWA results in additional outage probability.

For the MWA, we decompose the outage probability into two components. First, there is p^*_{out}, which is the minimum outage probability, corresponding the event that $P_s > P_{\max}$ and $v_i > P_{\max}$ for all $i > 0$. For the MWA, we have an additional outage probability, $p^{\text{M,g}}_{\text{out}}$, corresponding to realizations of the valuations which satisfy three conditions: that $P_s > P_{\max}$, that $\rho(\mathcal{V}) = 0$, and that there exists at least one i such that $v_i \leq P_{\max}$. Thus, the outage probability under the MWA, $p^{\text{m}}_{\text{out}} = p^*_{\text{out}} + p^{\text{M,g}}_{\text{out}}$. We have already mathematically characterized p^*_{out} in Eq. (9), and we now characterize the gap, $p^{\text{M,g}}_{\text{out}}$:

$$\begin{aligned}
p^{\text{M,g}}_{\text{out}} =& \Pr\left((P_s > P_{\max}) \bigcap \left(\cap_{i=1}^n c_i(v_i) > v_0\right) \bigcap \left(\cup_{i=1}^n v_i \leq v_0\right)\right) \\
=& \Pr\left(P_s > P_{\max}\right) \\
& \times \Pr\left(\left(\cap_{i=1}^n c_i(v_i) > v_0\right) \bigcap \left(\cup_{i=1}^n v_i \leq v_0\right) | P_s > P_{\max}\right) \\
=& \, p_{\text{out},s} \prod_{i=1}^n \left(F_{V_i}(P_{\max}) - F_{V_i}(\bar{v}_i)\right),
\end{aligned}$$

with $\bar{v}_i = c_i^{-1}(P_{\max})$, where, assuming regularity, c_i^{-1} is the well-defined inverse of the reverse auction virtual valuation function, $c_i(v_i)$.

Three circumstances reduce or eliminate the increased risk of outage. First, as long as a candidate wins the MWA, communication will occur, since the payment $X^M(\mathcal{V})$ will satisfy $X^M(\mathcal{V}) < c_{\rho^M}(X^M(\mathcal{V})) \leq v_0 \leq P_{\max}$. Secondly, if $P_s \leq P_{\max}$, then communication will always occur when possible, since even if the source wins, it is able to successfully transmit the data in time. Finally, as the number of candidates increases, the additional outage probability decreases. More specifically, if we again assume that candidates are independently and identically distributed (so that valuations, $v_i \; \forall i \in \mathcal{N}$ are i.i.d.), we have

$$p^{\text{M,g}}_{\text{out}} = P_{\text{out},s} \left(F_{V_c}(P_{\max}) - F_{V_c}(\bar{v}_c)\right)^n,$$

where the candidate-identifying subscript i has been replaced by c, denoting a generic candidate. This expression shows that the gap, $p^{\text{M,g}}_{\text{out}}$, between the minimum outage probability and the outage probability of the MWA decays exponentially in n. **Thus, we have shown that there is gap in outage probability between the cooperative baseline and the MWA, and that this gap decreases exponentially as the number of candidates increases.**

D. Energy Consumption

While the Myerson mechanism may result in a larger outage probability, it also reduces the average energy consumption. To build intuition as to why, consider a simple scenario with a single candidate, and assume that $v_1 < c_1(v_1) < v_0$. In the case of the VWA, the total source transmit power is $P_{\text{tot}} = v_0$, while for the MWA, we have $P_{\text{tot}} = c_1^{-1}(v_0) < v_0$. As numerical results in Section VI show, this difference can be significant.

In summary, the MWA increases energy efficiency but does so at the cost of a greater outage probability. We next present several numerical results which illustrate the analysis of the preceding sections.

VI. Numerical Results

We now present numerical studies illustrating the analysis presented in the previous sections. We compare the outage probability, the source energy usage, and the energy harvested using both the VWA and MWA under different fading assumptions. These showcase when one type of auction will be preferred over the other, as well as how the number of candidates, the fading characteristics, and the blockage geometry impact system performance. Where appropriate, we compare the results of the auction-based protocol to the cooperative lower bound and to an upper bound corresponding to the worst-case scenario where the relay service is not available, which we refer to as the source-only scenario.

Throughout the section, we consider the setup depicted in Fig. 3, with $q_s = (5.76\,\text{m}, 5.76\,\text{m})$, the AP at the origin, and a large circular blockage occluding the LOS path. The locations of the candidates, q_i, are i.i.d. uniformly across the regions where a LOS path exists to both the AP and source, i.e., the non-gray areas in Fig. 3 (a) and (b). We use the following system parameters, drawn from real-world studies for channels at 28 GHz: For LOS channels, we set the path loss intercept and exponent to $K^{\text{LOS}} = 0$ and $\eta^{\text{LOS}} = 2.5$, respectively, while for NLOS channels we set $K^{\text{NLOS}} = -25$ and $\eta^{\text{NLOS}} = 5.76$. Both lognormal and Rayleigh fading is considered, and the lognormal fading is parameterized with $\sigma_{\text{f, dB}} = 8.66$ for LOS channels and $\sigma_{\text{f, dB}} = 9.02$ for NLOS channels [2, Table VI], [46]. We set $\psi_f = 1/\sqrt{2}$ for all Rayleigh fading experiments to ensure that the same total power is used for the lognormal and Rayleigh cases. The receiver noise power is taken as $\sigma^2 = -75\,\text{dBm}$, and $P_{\max} = 100\,\text{mW}$. We consider a fixed time of $T = 1\,\text{s}$ and a bandwidth-normalized payload of $D = 8$ bits/Hz, so that the data must be sent at a rate of at least $r = 8$ bits/s/Hz. If the maximum achievable rate as defined in Eq. (1) is less than this on any of the channels used for communication, we declare an outage. For WPT, we take the circuity efficiency to be $\alpha = 0.2$ [47] and the effective aperture as $A_r = 0.01\,\text{m}^2$.

Analysis in the preceding sections assumes that the fading component of the channel is independent for each candidate, as fading decorrelates within a few wavelengths [41, 44], with larger-scale correlation due to shadowing captured through LOS/NLOS effects. However, for completeness, our simulations account for spatial correlation of the fading. For lognormal fading, we generate dB-domain samples by drawing from

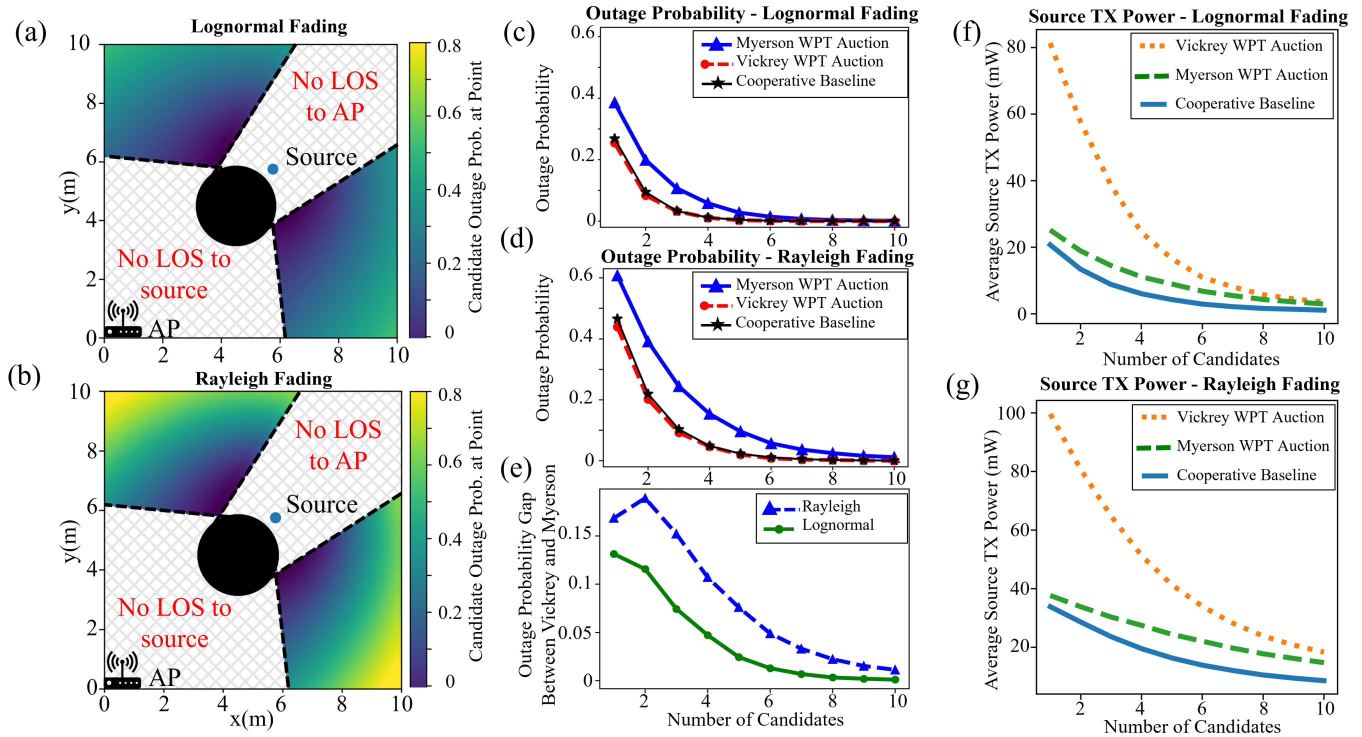

Fig. 3. Numerical results for a sample blockage scenario. (a) and (b): The probability that a candidate at each point could act as a relay in the cooperative case for (a) lognormal and (b) Rayleigh fading, i.e., $p_{\mathrm{out},c}$ from Eq. (8) conditioned on candidate placement. Areas which do not have a LOS path to both the AP and the source are crosshatched. (c) and (d): The outage probability of the MWA, VWA, and cooperative baseline for (c) lognormal and (d) Rayleigh fading. The cooperative baseline outage probability is calculated using the expression for the minimal outage probability in Eq. (9), while the MWA and VWA outage probabilities are determined empirically from the numerical experiments. The outage probability under the MWA is greater than it is for the VWA, which matches the minimum outage probability. For both the VWA and MWA, the outage probability decays exponentially. (e): The outage probability gap between the Vickrey and Myerson auction. This gap decays exponentially in the number of candidates. (f) and (g): The average source transmit power under the VWA and MWA, as well as for the cooperative baseline introduced in Section III, for (f) lognormal and (g) Rayleigh fading. Energy usage for the MWA is less than it is under the VWA, and energy efficiency converges as the number of candidates increases. See color PDF for optimal viewing.

a correlated normal distribution, where the covariance between fading at two points, q_i and q_j, is given by $\sigma^2(q_i, q_j) = \sigma^2_{\mathrm{f,\,dB}} \exp(-||q_i - q_j||/d_{\mathrm{dc}})$, with d_{dc} as the decorrelation distance [48]. In our experiments, we use $d_{\mathrm{dc}} = 0.1$ m. Similarly, following [44, 48], we generate correlated Rayleigh fading samples in the dB domain by independently sampling two correlated normal variables for the in-phase and quadrature components, using the covariance from [48, Eq. (25)]. The final channel fading values are obtained by summing their squared magnitudes. These channel simulations, along with the geometric calculations for LOS determination, are implemented in Python using standard scientific computing libraries.

Throughout, we show system performance with different numbers of candidates, under different fading models, and in different environments. For each combination of number of candidates, fading model, and environment geometry, we sample 10,000 different possible placements of the n candidates, and for each candidate we sample fading variables from the corresponding distribution. For each sampled problem instance, we calculate the cooperative baseline and the results of both the VWA and MWA. We report the average of these batches of 10,000 problem instances.

A. Outage Probability

We first study the outage probability across auction types, looking at the impact of the number of candidates and the fading characteristics. We first calculate the outage probability of the source using Eq. (7), which we find to be $p_{\mathrm{out,s}} = 0.76$ for lognormal fading and $p_{\mathrm{out,s}} = 0.99$ for Rayleigh fading. This is the source-only upper bound on outage probability, corresponding to the case where the source does not have the option to relay.

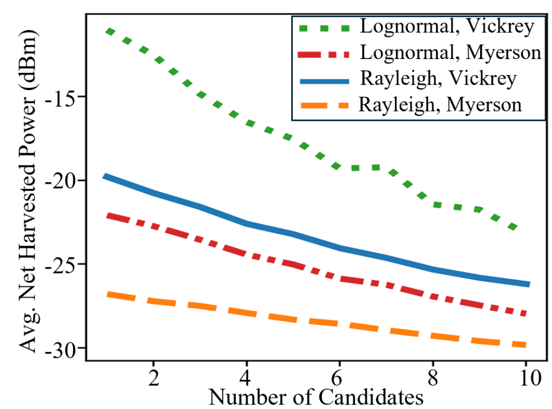

Fig. 4. Average net energy harvested for the scenario depicted in Fig. 3.

Averaging over the possible positions of the candidates as well as the possible realizations of the channel fading power, we find that the outage probability for an arbitrary agent, mathematically characterized in Eq. (8), is $p_{\mathrm{out,c}} = 0.35$ for lognormal fading and $p_{\mathrm{out,c}} = 0.47$ for Rayleigh fading (Fig. 3

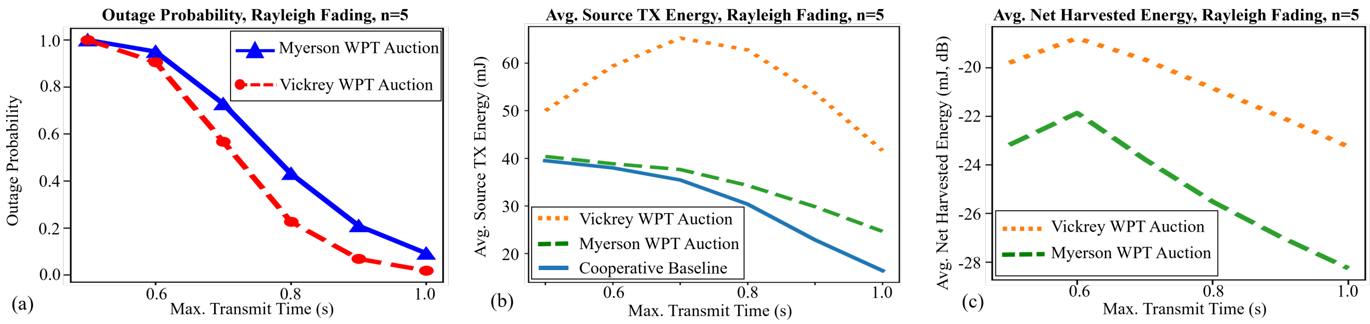

Fig. 5. Numerical results illustrating the impact of maximum transmit time, T, on system performance for a system of of $n = 5$ relay candidates under Rayleigh fading. (a): Impact of maximum transmit time on outage probability. The outage probability for the Myerson and Vickrey auctions decreases as the transmit time increases. As discussed in Section IV, the outage probability of the cooperative baseline is equal to that of the Vickrey auction. (b): Impact of maximum transmit time on average energy consumption. The average energy consumption, which generally decreases as the maximum transmit time increases. Interestingly, source energy consumption peaks around 65 mJ for the Vickrey auction with $T = 0.7$ s. (c): Impact of maximum transmit time on average net energy harvested. The net energy harvested peaks at $T = 0.6$ s, and generally, the source pays the relay candidate less when data offloading is less urgent (larger T).

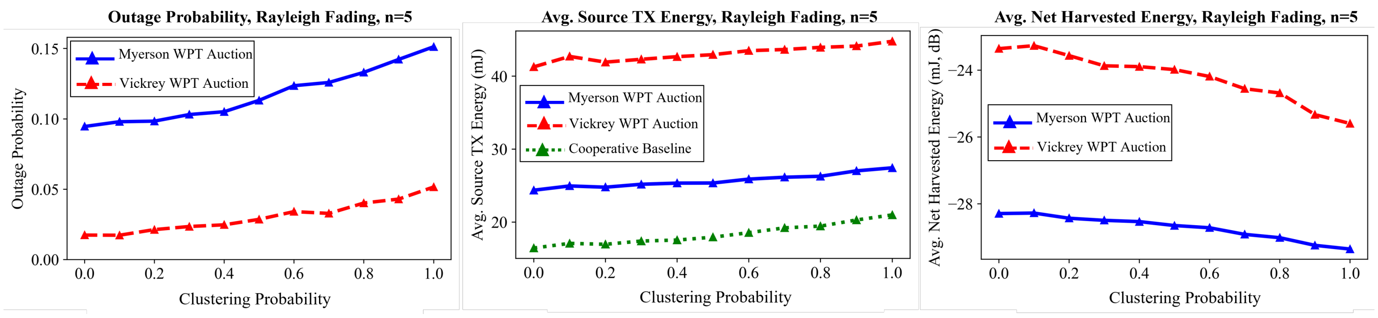

Fig. 6. Numerical results illustrating the impact of correlation probability, ξ, on system performance for a system of $n = 5$ relay candidates under Rayleigh fading. (a): Impact of correlation on outage probability. As points become more correlated and spatially concentrated, the outage probability increases due to decreased diversity in relay candidate locations. (b): Impact of correlation on source transmit power. Increased correlation modestly increases the average source transmit power. (c): Impact of correlation on average net energy harvested. Increased spatial clustering reduces the net energy harvested by the winning relay candidate.

(b)). Thus, we will see lower outage probabilities under lognormal fading than we see under Rayleigh fading, though we note that for different choices of variance σ_f^2, this relationship may not hold. These candidate outage probabilities are then used to calculate the minimum outage probability p^*_{out} using Eq. (9), which is compared to the outage probabilities of the VWA and MWA computed empirically from the simulation experiments. As stated in Lemma 1, we see that the VWA achieves the minimum outage probability, i.e., $p^*_{\text{out}} = p^V_{\text{out}}$, while there is a gap between the minimum outage probability and the outage probability of the MWA. The results also demonstrate the exponential decay predicted in our discussion in Sections IV, and Fig. 3 (e) shows that the gap in outage probability between the MWA and minimum outage probability decays exponentially, as discussed in Section V. Crucially, both the VWA and MWA reduce the outage probability by as much as 50% and 34%, respectively, with only a single relay candidate compared to the source-only upper bound, and both push the probability near 0 for larger values of n.

B. Source Energy Usage

Figs. 3 (f) and (g) compare the source's average energy consumption under both the VWA and MWA, with the cooperative scenario as a baseline. For fair comparison, we take averages for each of the methods only over cases with successful communication. We see that, as expected, the MWA results in significantly less energy usage than the VWA, and that for large n, the energy consumption of both auctions approaches that of the baseline. The decay in energy consumption is particularly pronounced for the VMA. Thus, while the VWA achieves a lower outage probability than the MWA, the MWA is more energy efficient. Both auction protocols significantly reduce energy usage compared to the source-only upper bound, which uses on average 85 mJ and 100 mJ under lognormal and Rayleigh fading, respectively. More specifically, with only a single available candidate, the MWA reduces average energy consumption by over 60%, while with as few as four available candidates, the VWA decreases the energy consumption of the source by 65%.

C. Energy Harvested

The average energy harvested by the candidates is plotted in Fig. 4. Increasing the number of candidates makes the auction more competitive, and consequently we see the energy harvested decreases. Similarly, the MWA reduces the net energy harvested by the candidates when compared to the VMA, as the MWA allocates more of the net energy savings of the system to the source. As discussed in earlier sections, the net energy harvested by the candidates is several orders of magnitude smaller than the energy used by the source, so that source energy consumption dominates considerations of energy efficiency in the system.

D. Impact on Transmit Time

We now investigate the impact of the maximum transmit time, T, on system performance. Specifically, we consider $T = 0.1k$ for $k \in 5, \ldots, 10$ in a system of $n = 5$ relay candidates with Rayleigh fading, and the corresponding results are presented in Fig. 5. As expected, we observe that increasing T generally reduces the outage probability and the source's transmit power for both the MWA and VWA, aligning with the intuition that a longer transmission window reduces the required transmit rate and therefore increases the likelihood of successful communication. However, for the VWA, the source's energy consumption reaches a peak of approximately 65 mJ at $T = 0.7$ s. This is because for $T < 0.7$ s, the source must almost always transmit at the maximum power ($P_{\max} = 100$ mW) when communication occurs, resulting in a linearly increasing relationship between maximum transmit time, T, and total energy consumption.

We also find that the energy harvested by the winning relay candidate exhibits a non-monotonic trend, peaking at $T = 0.6$ s. For, $T > 0.6$, the auction dynamics effectively results in the relay candidates gaining a premium for smaller values of T (more urgent communication). Conversely, when T is large, the urgency is reduced, and the source pays the relay less.

E. Impact of Spatial Distribution

Thus far, we have assumed that relay candidates are uniformly and independently distributed across the region of interest. However, in practical scenarios, relay locations may exhibit spatial correlation, forming clusters rather than being uniformly spread. To investigate this effect, we introduce a sampling procedure that generates spatially correlated relay distributions. First, we sample the initial relay candidate position, q_1, uniformly from the region with LOS to both the AP and the source. For each subsequent relay candidate, with clustering probability ξ, it is sampled from a Gaussian distribution centered at q_1 with a standard deviation of 0.5 m along each axis. Specifically, $q_i \sim \mathcal{N}(q_1, 0.25\, I_{2\times 2})$, where $I_{2\times 2}$ is the 2×2 identity matrix. We then use rejection sampling to ensure that these points maintain LOS to both the AP and the source. With probability $1-\xi$, the relay candidate is instead sampled uniformly from the region.

By varying the value of ξ, we can systematically study the impact of clustering on system performance. When $\xi = 0$, all relay candidates are independently and uniformly distributed, representing no clustering. Conversely, when $\xi = 1$, all relay candidates are drawn from a single Gaussian distribution whose mean is itself uniformly sampled from the region[5]. Intermediate values of ξ allow for a continuum between these two extremes, enabling controlled analysis of the impact of spatial correlation on system performance.

[5]This allows us to identify the impact of clustering independent of exactly where in the space the cluster is centered

Fig. 6 shows the results from the experiment in a system with $n = 5$ relay candidates under Rayleigh fading. Interestingly, increased spatial correlation degrades performance in terms of both outage probability and energy consumption, as it reduces diversity in relay candidate placement. Additionally, higher spatial correlation leads to a decrease in net energy harvested. This occurs because relay candidates clustered together experience similar channel conditions, resulting in comparable valuations. When the gap between the lowest and second-lowest valuations is smaller, the winning candidate harvests less energy.

F. Impact of Blockage Geometry

To better understand the impact of the environment, we consider an additional blockage configuration, shown in Fig. 7 (a), under Rayleigh fading. Due to the geometry of the blockages in this environment, the outage probability for an arbitrary candidate is $p_{\text{out,c}} = 0.36$, lower than it was in the blockage environment considered in Fig. 3 under Rayleigh fading, and comparing Fig. 7 (b) to Fig. 3 (d), we see that the outage probabilities drop more quickly in this environment than they do in the environment considered previously. Similarly, the average source TX power drops more quickly in this alternate blockage configuration (compare Fig. 7 (b) to Fig. 3 (g)). Thus, while the overall trends of rapid decay in outage probability and energy consumption are consistent across environments, certain blockage environments lead to better performance than others.

G. Comparing Auction Types

The previous results illustrate the inherent tradeoff between the VWA and MWA. For small n, the MWA provides significant energy savings compared to the VWA, but at the cost of a higher Outage probability. As n grows, the energy savings offered by the MWA become less dramatic. However, the outage probability gap, $p_{\text{out}}^{M,g}$, also shrinks.

To better understand when one auction type should be used instead of the other, we compare the average utility, U_s, as defined in Eq. (2) for both the MWA and VWA under Rayleigh fading in the environment shown in Fig. 3. Specifically, for each value of n, we find the value of C (the reward for successful communication in Eq. (2)) such that the source is indifferent between the two auctions and plot them in Fig. 8. As C grows larger, greater importance is placed on ensuring communication occurs, i.e., reducing outage probability, and energy efficiency becomes less critical. We therefore see that when ensuring communication is more important (larger values of C), the VWA is preferred, as it achieves the minimum outage probability. On the other hand, the MWA is preferred when greater importance is placed on energy efficiency (smaller values of C). Qualitatively, we see that as n increases, the MWA becomes preferred for a greater range of values of C. This suggests that as the number of candidates increases, the MWA becomes more desirable.

This article has been accepted for publication in IEEE Transactions on Wireless Communications. This is the author's version which has not been fully edited and content may change prior to final publication. Citation information: DOI 10.1109/TWC.2025.3563828

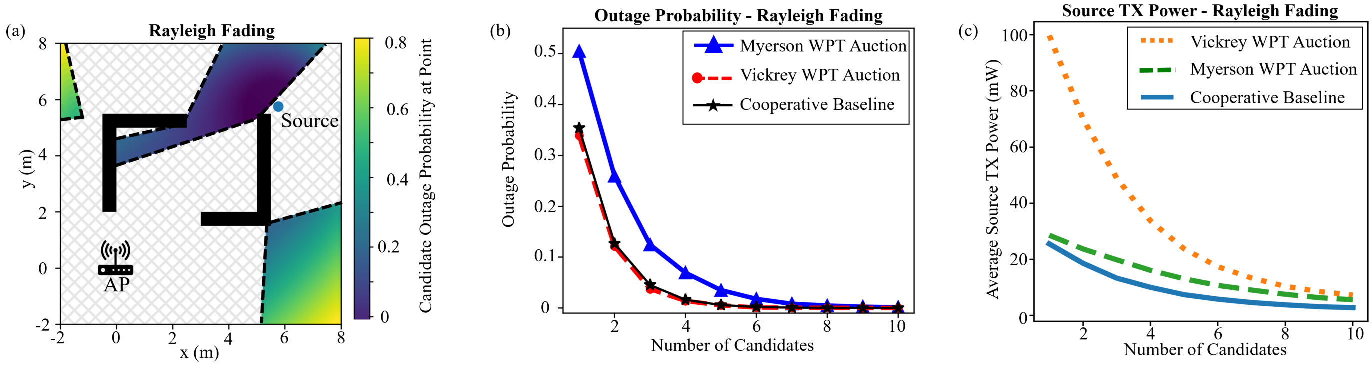

Fig. 7. Numerical results for the blockage scenario shown in (a) under Rayleigh fading. (a): The probability that a candidate at each point could act as a relay in the cooperative case,i.e., $p_{\text{out},c}$ from Eq. (8) conditioned on candidate placement. Areas which do not have a LOS path to both the AP and the source are crosshatched. (b): The empirical outage probability of the MWA and VWA, and the analytical outage probability of cooperative baseline, calculated using Eq. (9). (c): The average source transmit power under the VWA and MWA, as well as for the cooperative baseline introduced in Section III. See color PDF for optimal viewing.

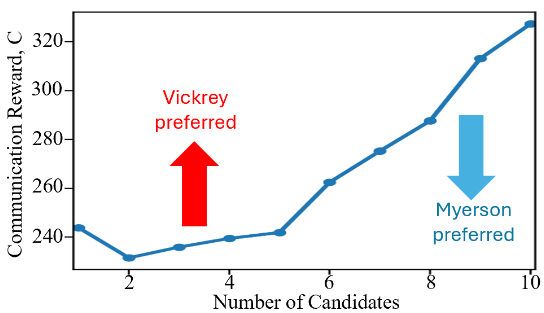

Fig. 8. Proposed design space: The blue line indicates the values of the communication reward, C, defined in Eq. (2), such that the source's expected utility is equal under the VWA and MWA. Conceptually, C is a penalty for failing to communicate. For values of C below the line, the MWA is preferred. For values of C above the line, the VWA is preferred.

H. Computational Complexity

We next compare the computation required for the VWA and MWA as well as for the cooperative lower bound. All three approaches require the same coordinating communication steps, outlined in Section III, and computationally, the difference in these protocols lie in the mechanisms (ρ^M, X^M), (ρ^V, X^V), and (ρ^C, X^C). Each of these runs in $O(n)$ time, as the source must compare the valuations or virtual valuations of each of the n relay candidates. In general, a Myerson auction could be computationally intensive due to the need to find the convex hull of virtual valuation functions. However, the key results in Theorems 2 and 3 prove the regularity of the auction under lognormal and Rayleigh fading, so that virtual valuations can be easily calculated.

VII. Conclusions and Future Work

This paper presents a novel approach to incentivizing non-cooperative, battery-powered UEs to act as relays through the use of wireless power transfer (WPT) and auction-based protocols. By analyzing the performance of Vickrey and Myerson auctions under realistic channel conditions, we have demonstrated that these mechanisms offer promising solutions for optimizing both energy efficiency and outage probability in non-cooperative relay networks with limited information. Through mathematical analysis and proofs, we have shown that the Vickrey WPT auction (VWA) achieves the same minimum outage probability achieved in the non-cooperative case, while the Myerson WPT auction (MWA) is an energy-efficient alternative at the cost of a possibly greater outage probability. Extensive numerical results corroborate our analytical findings and highlight the critical role of system parameters, such as the number of candidate UEs, the fading environments, and the geometry of the blockages. Overall, the mathematical analysis and numerical results provide guidance on when one auction type is preferred over the other.

Several directions remain open for future research. One avenue involves extending the MWA to handle non-regular Rician fading models. While the VWA applies to any fading model, our discussion of the MWA focused on lognormal and Rayleigh fading due to their analytical tractability. Incorporating "ironing" procedures [38] would make the MWA applicable to a broader range of fading environments.

Another important direction is introducing more dynamic adaptability into the system. This includes developing mechanisms to select between different auction types in real time based on network conditions and optimizing over transmission time T rather than treating it as a fixed parameter. Relaxing the constraint on T would allow for a more flexible and responsive auction framework, particularly in scenarios where strict timing constraints are not required. Furthermore, expanding the model to account for mobility would open new research directions, particularly in the context of communication-aware robotics [49]. Studying auctions with a mobile source or mobile relays introduces additional challenges related to link stability, power dynamics, and relay selection.

Finally, revisiting assumptions related to the UEs' utility could lead to intriguing avenues for future work. For example, the impact of non-winning candidates harvesting energy from the source's transmission warrants deeper investigation, and understanding how passive energy harvesting affects bidding strategies and overall network efficiency could lead to refinements in the auction design. Hybrid incentive systems that combine energy-based payments with monetary or alternative incentives could also offer a more comprehensive understanding of system performance, making auction-based relaying more applicable to real-world deployments.

Appendix A
Proof of Corollary 1

Proof. Our proof consists of two parts. First, we show that Definitions 2 and 3 are equivalent. Then, we show that the two mechanisms are equivalent as well. We first cast the reverse auction as a forward auction by negating the valuations. Let $v_i^f = -v_i$ denote the equivalent forward auction valuations. Then we have

$$\begin{aligned} c_i^f(v_i^f) = c_i^f(-v_i) &= -v_i - \frac{1 - F_{V_i^f}(-v_i)}{f_{V_i^f}(-v_i)} \\ &= -v_i - \frac{F_{V_i}(v_i)}{f_{V_i}(v_i)} = -c_i(v_i). \end{aligned} \tag{13}$$

Thus, $c_i(v_i)$ corresponds to the negation of the forward auction virtual valuations. Furthermore, we note that

$$\frac{dc_i^f(v_i^f)}{dv_i^f} = \frac{(-1)dc_i(v_i)}{(-1)dv_i} = \frac{dc_i(v_i)}{dv_i}.$$

Therefore, the valuations of the reverse auction satisfy the condition in Definition 3 if and only if the valuations of the equivalent forward auction satisfy Definition 2.

We must also show that the reverse auction and forward auction mechanisms are equivalent, i.e., $\rho^M(\mathcal{V}) = \rho^{f,M}(-\mathcal{V})$ and $X^M(\mathcal{V}) = -X^{f,M}(-\mathcal{V})$, where $-\mathcal{V}$ is the set of valuations in the equivalent forward auction. This follows directly from the negation of the virtual valuations shown in Eq. (13) and the definitions of the mechanisms in Eq. (10) and Eq. (11).

Appendix B
Proof of Theorem 2

Proof. As a general statement, we have

$$\begin{aligned} \frac{d\tilde{c}_i(\tilde{v}_i)}{d\tilde{v}_i} &= 1 + \frac{f_{\tilde{V}_i}(\tilde{v}_i)}{f_{\tilde{V}_i}(\tilde{v}_i)} - \frac{F_{\tilde{V}_i}(\tilde{v}_i)}{f_{\tilde{V}_i}(\tilde{v}_i)^2}\frac{df_{\tilde{V}_i}(\tilde{v}_i)}{d\tilde{v}_i} \\ &= 2 - \frac{F_{\tilde{V}_i}(\tilde{v}_i)}{f_{\tilde{V}_i}(\tilde{v}_i)^2}\frac{df_{\tilde{V}_i}(\tilde{v}_i)}{d\tilde{v}_i}. \end{aligned} \tag{14}$$

For lognormal shadowing, the CDF of the fading is $F_{H_f^{\text{LOS}}}(h) = \Phi(\ln(h)/\sigma_f)$, with $\Phi(\cdot)$ the CDF of the standard normal distribution, while the PDF is $f_{H_f^{\text{LOS}}}(h) = \frac{1}{h\sigma_f\sqrt{2\pi}}\exp(-\ln(h)/2\sigma_f^2)$. Based on this, we have

$$F_{\tilde{V}_i}(\tilde{v}_i) = 1 - \Phi\left(\frac{\ln(h_i(\tilde{v}_i))}{\sigma_{\text{f}}}\right)$$

and

$$f_{\tilde{V}_i}(\tilde{v}_i) = \frac{dF_{\tilde{V}_i}(\tilde{v}_i)}{d\tilde{v}_i} = \frac{h_i(\tilde{v}_i)}{C_i\sigma_f\sqrt{2\pi}}\exp\left(\frac{-\ln(h_i(\tilde{v}_i))}{2\sigma_f^2}\right).$$

Differentiating, we get

$$\begin{aligned} \frac{df_{\tilde{V}_i}(\tilde{v}_i)}{d\tilde{v}_i} &= \frac{df_{\tilde{V}_i}(\tilde{v}_i)}{dh_i(\tilde{v}_i)}\frac{dh_i(\tilde{v}_i)}{d\tilde{v}_i} \\ &= \frac{\exp(-\ln h_i(\tilde{v}_i)/(2\sigma_f^2))}{C_1\sigma_f\sqrt{2\pi}}\left(1 - \frac{\ln h_i(\tilde{v}_i)}{\sigma_f^2}\right)\frac{-C_i}{\tilde{v}_i^2} \\ &= \frac{-\exp(-\ln h_i(\tilde{v}_i)/(2\sigma_f^2))}{\tilde{v}_i^2\sigma_f\sqrt{2\pi}}\left(1 - \frac{\ln h_i(\tilde{v}_i)}{\sigma_f^2}\right) \\ &= \frac{-f_{\tilde{V}_i}(\tilde{v}_i)}{\tilde{v}_i}\left(1 - \frac{\ln h_i(\tilde{v}_i)}{\sigma_f^2}\right). \end{aligned}$$

We can now expand Eq. (14):

$$\begin{aligned} \frac{d\tilde{c}_i(\tilde{v}_i)}{d\tilde{v}_i} &= 2 - \frac{F_{\tilde{V}_i}(\tilde{v}_i)}{f_{\tilde{V}_i}(\tilde{v}_i)^2}\frac{-f_{\tilde{V}_i}(\tilde{v}_i)}{\tilde{v}_i}\left(1 - \frac{\ln h_i(\tilde{v}_i)}{\sigma_f^2}\right) \\ &= 2 + \frac{F_{\tilde{V}_i}(\tilde{v}_i)}{f_{\tilde{V}_i}(\tilde{v}_i)\tilde{v}_i}\left(1 - \frac{\ln h_i(\tilde{v}_i)}{\sigma_f^2}\right) \\ &= 2 + \frac{F_{\tilde{V}_i}(\tilde{v}_i)}{f_{H_{\text{f}}}(h_i(\tilde{v}_i))h_i(\tilde{v}_i)}\left(1 - \frac{\ln h_i(\tilde{v}_i)}{\sigma_f^2}\right) \\ &= 2 + \frac{1 - \Phi\left(\frac{\ln h_i(\tilde{v}_i)}{\sigma_f}\right)}{\phi\left(\frac{\ln h_i(\tilde{v}_i)}{\sigma_f}\right)\sigma_f^{-1}}\left(1 - \frac{\ln h_i(\tilde{v}_i)}{\sigma_f^2}\right). \end{aligned}$$

We then let $\gamma = \ln(h_i(\tilde{v}_i))/\sigma_f$ to get

$$\frac{d\tilde{c}_i(\tilde{v}_i)}{d\tilde{v}_i} = 2 + \frac{1 - \Phi(\gamma)}{\phi(\gamma)}\left(\sigma_f - \gamma\right).$$

where ϕ is the PDF of the standard normal distribution. We note that $(1 - \Phi(\gamma))/\phi(\gamma)$ is by definition the Mills ratio for a standard normal distribution, for which the following inequality holds [50]: $(1 - \Phi(\gamma))/\phi(\gamma) < 1/\gamma,\ \forall\gamma > 0$. Consequently, for all $\tilde{v}_i$, we have $d\tilde{c}_i(\tilde{v}_i)/d\tilde{v}_i > 0$.

References

[1] ITU-R, "Framework and overall objectives of the future development of IMT for 2030 and beyond," ITU-R, Tech. Rep., 2023, Draft New Recommendation.

[2] I. A. Hemadeh, K. Satyanarayana, M. El-Hajjar, and L. Hanzo, "Millimeter-Wave Communications: Physical Channel Models, Design Considerations, Antenna Constructions, and Link-Budget," *IEEE Commun. Surveys & Tutorials*, vol. 20, no. 2, pp. 870–913, 2018.

[3] D. C. Nguyen, M. Ding, P. N. Pathirana, A. Seneviratne, J. Li, D. Niyato, O. Dobre, and H. V. Poor, "6g internet of things: A comprehensive survey," *IEEE Internet of Things J.*, vol. 9, no. 1, pp. 359–383, 2022.

[4] C.-X. Wang, X. You, X. Gao, X. Zhu, Z. Li, C. Zhang, H. Wang, Y. Huang, Y. Chen, H. Haas, J. S. Thompson, E. G. Larsson, M. D. Renzo, W. Tong, P. Zhu, X. Shen, H. V. Poor, and L. Hanzo, "On the road to 6g: Visions, requirements, key technologies, and testbeds," *IEEE Commun. Surveys & Tutorials*, vol. 25, no. 2, pp. 905–974, 2023.

[5] T. D. Ponnimbaduge Perera, D. N. K. Jayakody, S. K. Sharma, S. Chatzinotas, and J. Li, "Simultaneous wireless information and power transfer (swipt): Recent advances and future challenges," *IEEE Commun. Surveys & Tutorials*, vol. 20, no. 1, pp. 264–302, 2018.

[6] S. Özyurt, A. F. Coşkun, S. Büyükçorak, G. Karabulut Kurt, and O. Kucur, "A survey on multiuser swipt commun. for 5g+," *IEEE Access*, vol. 10, pp. 109 814–109 849, 2022.

[7] R. Kamran, S. Kiran, P. Jha, A. Karandikar'T, and P. Chaporkar, "Green 6g: Energy awareness in design," in *2024 16th Int. Conf. on COMmunication Systems & NETworkS (COMSNETS)*, 2024, pp. 1122–1125.

[8] J. Van Mulders, D. Delabie, C. Lecluyse, C. Buyle, G. Callebaut, L. Van der Perre, and L. De Strycker, "Wireless power transfer: Systems, circuits, standards, and use cases," *Sensors (Basel)*, 2022.

[9] L. Xie, X. Cao, J. Xu, and R. Zhang, "Uav-enabled wireless power transfer: A tutorial overview," *IEEE Trans. on Green Commun. and Networking*, vol. 5, no. 4, pp. 2042–2064, 2021.

[10] M. Cansiz, D. Altinel, and G. K. Kurt, "Efficiency in RF energy harvesting systems: A comprehensive review," *Energy*, vol. 174, pp. 292–309, 2019. [Online]. Available: https://www.sciencedirect.com/science/article/pii/S0360544219302993

[11] S. Kim, R. Vyas, J. Bito, K. Niotaki, A. Collado, A. Georgiadis, and M. M. Tentzeris, "Ambient rf energy-harvesting technologies for self-sustainable standalone wireless sensor platforms," *Proceedings of the IEEE*, vol. 102, no. 11, pp. 1649–1666, 2014.

[12] S. A. Fallahpour, S. Karimian, and E. Mehrshahi, "Design of a high-efficiency rf energy harvesting system," in *2022 30th Int. Conf. on Electrical Engineering (ICEE)*, 2022, pp. 920–925.

[13] I. D. Bougas, M. S. Papadopoulou, A. D. Boursianis, P. Sarigiannidis, S. Nikolaidis, and S. K. Goudos, "Energy harvesting & autonomous energy systems: A proposal for rf energy harvesting," in *2024 13th Int. Conf. on Modern Circuits and Systems Technologies (MOCAST)*, 2024, pp. 1–5.

[14] X. Li, Q. Wang, M. Liu, J. Li, H. Peng, M. J. Piran, and L. Li, "Cooperative Wireless-Powered NOMA Relaying for B5G IoT Networks With Hardware Impairments and Channel Estimation Errors," *IEEE Internet of Things J.*, vol. 8, no. 7, pp. 5453–5467, 2021.

[15] H. Liu, K. J. Kim, K. S. Kwak, and H. Vincent Poor, "Power Splitting-Based SWIPT With Decode-and-Forward Full-Duplex Relaying," *IEEE Trans. on Wireless Commun.*, vol. 15, no. 11, pp. 7561–7577, 2016.

[16] C. Zhai, Y. Li, and L. Qiao, "Wireless Power Transfer Based Adaptive Relaying With Energy Accumulation," *IEEE Trans. on Veh. Technol.*, vol. 69, no. 10, pp. 11 014–11 027, 2020.

[17] M. A. Hossain, R. Md Noor, K.-L. A. Yau, I. Ahmedy, and S. S. Anjum, "A Survey on Simultaneous Wireless Information and Power Transfer With Cooperative Relay and Future Challenges," *IEEE Access*, vol. 7, pp. 19 166–19 198, 2019.

[18] G. A. Ropokis and P. S. Bithas, "Wireless powered relay networks: Rate optimal and power consumption-aware wpt/swipt," *IEEE Trans. on Veh. Technol.*, vol. 71, no. 8, pp. 8574–8590, 2022.

[19] N. Ashraf, S. A. Sheikh, S. A. Khan, I. Shayea, and M. Jalal, "Simultaneous wireless information and power transfer with cooperative relaying for next-generation wireless networks: A review," *IEEE Access*, vol. 9, pp. 71 482–71 504, 2021.

[20] H. Lee, B. Lee, H. Yang, J. Kim, S. Kim, W. Shin, B. Shim, and H. V. Poor, "Towards 6g hyper-connectivity: Vision, challenges, and key enabling technologies," *Journal of Communications and Networks*, vol. 25, no. 3, 2023.

[21] B. T. Tinh, L. D. Nguyen, H. H. Kha, and T. Q. Duong, "Practical optimization and game theory for 6g ultra-dense networks: Overview and research challenges," *IEEE Access*, vol. 10, 2022.

[22] Z. Han, D. Niyato, W. Saad, T. Basar, and A. Hjorungnes, *Game Theory in Wireless and Communication Networks: Theory, Models, and Applications*. Cambridge University Press, 2012.

[23] A. Muralidharan and Y. Mostofi, "Path Planning for Minimizing the Expected Cost Until Success," *IEEE Trans. on Robotics*, vol. 35, no. 2, pp. 466–481, 2019.

[24] Y. Zeng, S. Chen, Y. Cui, J. Yang, and Y. Fu, "Joint resource allocation and trajectory optimization in uav-enabled wirelessly powered mec for large area," *IEEE Internet of Things Journal*, vol. 10, no. 17, pp. 15 705–15 722, 2023.

[25] H. Zhang, J. Du, J. Cheng, K. Long, and V. C. M. Leung, "Incomplete CSI Based Resource Optimization in SWIPT Enabled Heterogeneous Networks: A Non-Cooperative Game Theoretic Approach," *IEEE Trans. on Wireless Commun.*, vol. 17, no. 3, pp. 1882–1892, 2018.

[26] H. Chen, Y. Jiang, Y. Li, Y. Ma, and B. Vucetic, "A game-theoretical model for wireless information and power transfer in relay interference channels," in *2014 IEEE Int. Symposium on Information Theory*, 2014, pp. 1161–1165.

[27] Z. Ding, S. M. Perlaza, I. Esnaola, and H. V. Poor, "Power allocation strategies in energy harvesting wireless cooperative networks," *IEEE Trans. on Wireless Commun.*, vol. 13, no. 2, pp. 846–860, 2014.

[28] Y. Chen, Y. Zhao, Y. Ge, and C.-Z. Xu, "Game-theoretic power allocation scheme of cooperative localization in hybrid active–passive wireless sensor networks," *IEEE Internet of Things Journal*, vol. 11, no. 18, pp. 30 027–30 039, 2024.

[29] D. Das, R. K. Khadanga, and D. K. Rout, "A matching game framework for users clustering and resource allocation with wireless power transfer in a cr-noma network," *International Journal of Communication Systems*, vol. 36, no. 2, p. e5376, 2023. [Online]. Available: https://onlinelibrary.wiley.com/doi/abs/10.1002/dac.5376

[30] Y.-W. Chan, C.-M. Shih, and F.-T. Chien, "Enhancing content caching in d2d networks: A stackelberg game approach with wireless energy transfer and social awareness," *IEEE Access*, vol. 13, pp. 26 765–26 781, 2025.

[31] Y. Ni, S. Zhou, Q. Wang, Y. Zhou, and H. Zhu, "Auction Game Based Phone-to-Phone Electricity Trading via Wireless Energy Transfer," in *2019 IEEE 19th Int. Conf. Commun. Technol (ICCT)*, 2019, pp. 1213–1219.

[32] Y. Cheng, H. Zhao, Y. Ni, W. Xia, L. Yang, and H. Zhu, "A game-theoretic incentive mechanism for battery saving in full duplex mobile edge computing systems with wireless power transfer," *IEEE Trans. on Network and Service Management*, vol. 20, no. 3, pp. 3474–3486, 2023.

[33] A. K. Gupta, S. Ghosh, and M. R. Bhatnagar, "Pricing based scheme for uav-enabled wireless energy transfer," *IEEE Transactions on Vehicular Technology*, vol. 71, no. 12, 2022.

[34] A. K. Gupta and M. R. Bhatnagar, "A non-cooperative pricing strategy for uav-enabled charging of wireless sensor network," *IEEE Transactions on Green Communications and Networking*, 2024.

[35] H. Xu, H. Hui, C. Zhou, G. Zeng, and Z. Han, "Cooperative energy trading for hetnets with renewable energy: A dynamic energy trading game," *IEEE Internet of Things Journal*, vol. 11, no. 7, pp. 11 606–11 618, 2024.

[36] M. Li, S. He, and K. Wang, "An auction-based relay selection and power allocation scheme for cooperative wireless sensor networks," in *2020 Chinese Automation Congress (CAC)*, 2020.

[37] W. Vickrey, "Counterspeculation, Auctions, and Competitive Sealed Tenders," *The Journal of Finance*, vol. 16, no. 1, pp. 8–37, 1961.

[38] R. B. Myerson, "Optimal Auction Design," *Mathematics of Operations Research*, vol. 6, no. 1, pp. 58–73, 1981.

[39] N. Nisan, T. Roughgarden, E. Tardos, and V. Vazirani, *Algorithmic Game Theory*. Cambridge University Press, 2007.

[40] W. Hurst, A. Pallaprolu, and Y. Mostofi, "Emergent cooperation for energy-efficient connectivity via wireless power transfer," in *2024 IEEE Global Commun. Conference (GLOBECOM)*, accepted.

[41] M. K. Samimi, G. R. MacCartney, S. Sun, and T. S. Rappaport, "28 GHz Millimeter-Wave Ultrawideband Small-Scale Fading Models in Wireless Channels," in *2016 IEEE 83rd Veh. Technol. Conf. (VTC Spring)*, 2016, pp. 1–6.

[42] B. Prabhakar, E. Uysal Biyikoglu, and A. El Gamal, "Energy-efficient transmission over a wireless link via lazy packet scheduling," in *Proceedings IEEE INFOCOM 2001. Conference on Computer Communications. Twentieth Annual Joint Conference of the IEEE Computer and Communications Society (Cat. No.01CH37213)*, vol. 1, 2001, pp. 386–394 vol.1.

[43] X. Zhou, R. Zhang, and C. K. Ho, "Wireless information and power transfer: Architecture design and rate-energy tradeoff," in *2012 IEEE Global Commun. Conf. (GLOBECOM)*, 2012, pp. 3982–3987.

[44] A. Goldsmith, *Wireless Communications*. Cambridge University Press, 2009.

[45] S. Lu, F. Liu, Y. Li, K. Zhang, H. Huang, J. Zou, X. Li, Y. Dong, F. Dong, J. Zhu, Y. Xiong, W. Yuan, Y. Cui, and L. Hanzo, "Integrated sensing and communications: Recent advances and ten open challenges," *IEEE Internet of Things J.*, vol. 11, no. 11, pp. 19 094–19 120, 2024.

[46] H. Zhao, R. Mayzus, S. Sun, M. Samimi, J. K. Schulz, Y. Azar, K. Wang, G. N. Wong, F. Gutierrez, and T. S. Rappaport, "28 ghz millimeter wave cellular communication measurements for reflection and penetration loss in and around buildings in new york city," in *2013 IEEE Int. Conf. on Commun. (ICC)*, 2013, pp. 5163–5167.

[47] E. Kwiatkowski, C. T. Rodenbeck, T. Barton, and Z. Popović, "Power-combined rectenna array for x-band wireless power transfer," in *2020 IEEE/MTT-S Int. Microwave Symposium (IMS)*, 2020, pp. 992–995.

[48] A. Gonzalez-Ruiz, A. Ghaffarkhah, and Y. Mostofi, "A Comprehensive Overview and Characterization of Wireless Channels for Networked Robotic and Control Systems," *Journal of Robotics*, vol. 5, p. 19, 2011.

[49] W. Hurst, S. Evmorfos, A. Petropulu, and Y. Mostofi, "Unmanned vehicles in 6g networks: A unifying treatment of problems, formulations, and tools," 2024. [Online]. Available: https://arxiv.org/abs/2404.14738

[50] R. D. Gordon, "Values of Mills' Ratio of Area to Bounding Ordinate and of the Normal Probability Integral for Large Values of the Argument," *The Ann. of Mathematical Statistics*, vol. 12, no. 3, pp. 364–366, 1941.